National and Kapodistrian
University of Athens
Faculty of Biology
Department of Botany

BACHELOR THESIS

The cytoplasmic C-terminal region of NCS1/FUR transporters has a dual role in endocytosis and transport

Georgia Papadaki | 1113201200092

Supervisor:
George Diallinas
Professor of Molecular Microbiology

Athens, 2017

Εθνικό και Καποδιστριακό
Πανεπιστήμιο Αθηνών
Τμήμα Βιολογίας
Τομέας Βοτανικής

ΔΙΠΛΩΜΑΤΙΚΗ ΕΡΓΑΣΙΑ

Ο διττός ρόλος του καρβοξυτελικού άκρου στην ενδοκύτωση και στη λειτουργία των NCS1/FUR μεταφορέων

Γεωργία Παπαδάκη | 1113201200092

Επιβλέπων:
Γεώργιος Διαλλινάς
Καθηγητής Μοριακής Μικροβιολογίας

Αθήνα, 2017

Acknowledgements

I would like to express my gratitude to my supervisor Prof George Diallinas, who gave me the opportunity to work in his lab. His enthusiasm and passion for science are, I believe, rare characteristics and I feel privileged to have worked under his supervision. His willingness to provide valuable insight has helped me evolve not only scientifically, but also personally. Finally, I wish to thank him for believing in me and my dreams, and for providing generously the opportunity to work abroad.

I am indebted to Dr Sotiris Amillis for his constructive scientific guidance and personal advice, for always being there and for continuing this work. I particularly want to thank PhD candidate Olga Martzoukou for her help and encouragement, especially during the last few months of intense fatigue.

I would like to thank former lab members, Sophia Balaska, Georgia Sioupouli, Koar Khorozian, George Kapetanakis, Giannis Bartzokas as well as current lab members Martha Tselika, Anzie Kourkoulou, Vivian Tsouvali and Christina Biamis. I especially like to express my appreciation to Sophia Balaska for her continuous support. A special reference to all members of the Department of Botany for their kind support and generosity.

I would like to thank Charoula Peta, my collegue and dear friend, who helped me and stood there for me. I am also grateful for Ioanna Myronidi, who helped me more than she can imagine even from that far.

I owe special thanks to Neofytos Komninos, for his patience, caring and peerless sense of humor which helped me more times than I can recall. I feel very lucky to have people like him in my life.

Finally, I would like to thank my sister Myrto and my parents Filippos and Mania for their love and encouragement through all these years, and for believing in me, even in times of discouragement.

Table of Contents

1. Introduction

1.1 Ascomycota

1.1.1. Basic Features

Ascomycota is the largest phylum of the Fungi Kingdom, consisting of more than 6300 genera and 64000 species ranging from unicellular yeasts to fairly large morels and truffles, as well as some of the common black and green moulds, the powdery mildews and the cup fungi (Kirk *et al.*, 2008).

The primary morphological feature that distinguishes members of Ascomycota from all other fungi is the ascus, a saclike cell containing the ascospores, which are produced by a combination of meiosis and a subsequent mitotic division (Alexopoulos et al., 1996). Eight ascospores are typically formed within the ascus, although this number may vary according to the species and may be as little as one ascospore per ascus (Esser and Stahl, 1976). Asci are usually produced in fruiting bodies called ascocarps, also known as ascomata. Apart from this sexual cycle of reproduction, conidiospores are formed as a result of mitosis and are released in large numbers, allowing the fungus to disperse over a wide area.

Filamentous ascomycetes are characterized by a compartmentalized mycelium with distinctive walls called septa. Septa generate from the hyphal periphery and advance towards the centre, where a small circular pore is formed, through which the plasma membrane (PM) and cytoplasm extend, and nuclei are permitted to migrate from one hyphal compartment to the next (Alexopoulos et al., 1996).

Based on a series of major phylogenetic studies, the phylum Ascomycota is divided in three subphyla, the Pezizomycotina (Ascomycotina), containing almost all ascomycetes that produce ascocarps, the Saccharomycotina, consisting of most of the true yeasts, and the basal group Taphrinomycotina (Lutzoni et al., 2004; Kirk et al., 2008). Nevertheless, fruit body-based taxa names are still occasionally used.

1.1.2. Ecology and importance of Ascomycota

Ascomycetes rival other groups of eukaryotic organisms in their ability to occupy a broad range of habitats. Corticolous, lignicolous, foliicolous, coprophilous and marine ascomycetes are present in ecosystems worldwide, even at some of the most extreme environments on earth, such as the inside of rocks on the frozen plains of Antarctica. A few are entirely hyphogean, while others form long-lived symbiotic associations with green algae or cyanobacteria (lichens), as well as with plants (mycorrhizae) and animals. They are important decomposers and have substantial

roles in nutrient cycling, since they can break down large molecules, such as cellulose and lignin (Schoch et al., 2009).

Ascomycetes are also very important for food production. The fermentative ability of certain yeasts is the basis of the baking and brewing industries . The enzymes produced by some species of the genus Penicillium play a significant role in the manufacture of the famous French cheeses Camembert, Brie and Roquefort, while Aspergilli have been used since more than 2000 years in the orient for the production of local specialties, such as soyu (soy sauce), miso (fermented soybean paste) and sake (rice wine) (Scazzocchio, 2009). Morels (Morchella) and truffles (Tuber) are also known as some of the most sought-after fungi delicacies.

A huge array of metabolic products, such as antibiotics, organic acids, enzymes and vitamins, is provided by ascomycetes. The most famous case is that of penicillin, an antibiotic which triggered a revolution in the treatment of bacterial infectious diseases in the 20th century. Moreover, some species can be genetically engineered to produce useful proteins, such as insulin produced in Saccharomyces cerevisiae (Kjeldsen, 2000) and human growth hormone in Pichia pastoris (Apte-Deshpande et al., 2009).

However, along with their benefits and positive contributions, ascomycetes can also be very harmful. Some secondary metabolites secreted by them are responsible for food contaminations, which result in food spoilage and in some cases may lead to fatal intoxications (Scazzocchio, 2009). One of the most toxic and carcinogenic compounds known is the mycotoxin aflatoxin B1, produced by Aspergillus flavus. Furthermore, ascomycetes are widespread plant pathogens, causing great economic damages in agriculture (Dutch elm disease, powdery mildew), but are also responsible for animal and human infections, such as candidiasis (Candida albicans) and several dermatophyte (Epidermophyton floccosum) skin diseases (Berbee, 2001). Aspergilli are important opportunistic pathogens of individuals with compromised immune systems, causing a group of diseases collectively known as aspergilloses.

Finally, fungi are eukaryotes, more closely related to matazoans than plants; this is why ascomycetes can be useful models in molecular and cell biology (Scazzocchio, 2009). Moreover, several species have biological properties and genetic systems that make them ideally suited for basic biological research. Among them, S. cerevisiae and A. nidulans hold prominent positions in this field (Alexopoulos et al., 1996).

1.2 *Aspergillus nidulans*

1.2.1 Basic features

Aspergilli are homothallic, filamentous fungi belonging to the phylum Ascomycota. This genus was first described in 1729 by the Italian priest and botanist Pietro

Antonio Micheli and was named after an instrument called Aspergillum, which was used in the Roman Catholic mass to sprinkle holy water over the heads of the faithful (Scazzocchio, 2009).

The modern classification of Ascomycota, places A. nidulans in the subphylum Pezizomycotina, class of Eurotiomycetes, order Eurotiales and family Aspergillaceae. Furthermore, unlike the past classification of A. nidulans as the telomorph of Emericella nidulans, the single named but pleomorphic nomenclatural and taxonomical system classifies both anamorphic and telomorphic states in Aspergillus, while Emericella is considered synonymus to the latter (Houbraken et al., 2014).

*Aspergillus nidulans*is commonly isolated from soil, plant debris and house dust, and is an opportunistic pathogen of immunocompromised individuals. It is recognized by its distinct conidiophores terminated by a swollen vesicle bearing flask-shaped phialides, which are born on the intervening metulae. Conidia are produced in long chains, budding from the ends of the phialides, and have a green pigment in the wild type strain. The hyphal compartment that branches to give rise to the conidiophore is the foot cell. A. nidulans is normally haploid, but can be induced to grow as heterokaryon or vegetative diploid. It produces asexual conidiospores for rapid distribution in the environment and sexual ascospores for long-term survival in soil. The asci contain the ascospores and are dispersed in cleistothecia, which are surrounded by thick-walled nurse cells called “hülle cells” (Figure 1.1).

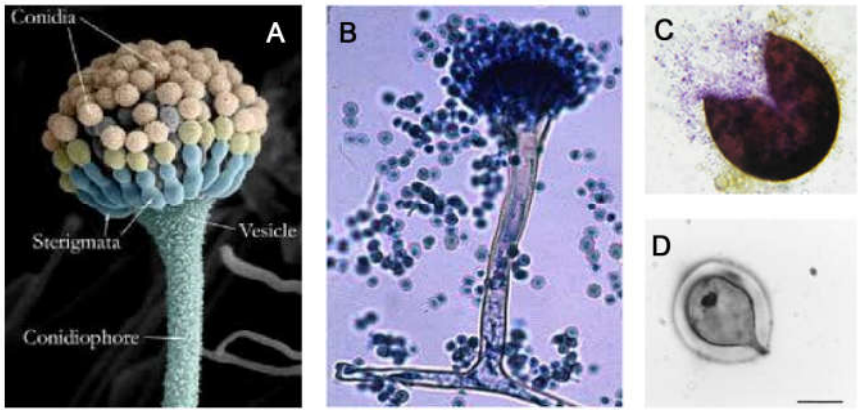

Figure 1.1 A-B. *Asexual conidiospores of Aspergillus nidulans****C.*** *Cleistothecium* ***D.*** *Hülle cells.*

1.2.2 Aspergillus nidulans as a model organism

A. nidulans has many advantages as a model organism, especially due to the fact that is well-studied in aspects of reproduction and metabolism. It has eight sequenced chromosomes with many auxotrophic, drug resistance and color markers. It is homothallic fungi, which means that there are no mating types and thus any two strains can be mated. It is normally haploid but heterokaryons and stable diploids can

be produced under stress, enabling the complementation analysis for mutations. Moreover, it grows rapidly on inexpensive media under a variety of nutritional conditions and produces conidia or ascospores that can be stored for long periods of time. It can be transformed in an integrative and site-specific manner and can generate stable transformants.

The conidiospores are in haploid form, which enables the direct screening of mutants or transformants by plating on appropriate media. Furthermore, by using different media or growth conditions we are able to detect mutations which lead to differential colony phenotypes related to diameter, thickness and color of conidiospores, characteristics that can also differ due to loss of function of a sole gene. For instance, *yA* gene encoding for lactase 1, an enzyme related to the color of conidiospores, is activated in specific developmental stages and structures facilitating the characterization of biochemical pathways.

Finally, *A. nidulans* is closely related to many other *Aspergillus* species which are of medical and industrial interest, such as *A. flavus, A. oryzae, A. niger* and *A. fumigatus,* and are exploited experimentally using technologies developed for *A. nilulans* (Scazzocchio, 2006).

1.3 Nutrient transport across the plasma membrane

1.3.1 Membrane proteins and transport

Biological membranes are indispensable to the life of the cell, as they define its boundaries and ensure the controlled communication between the cytosol and the extracellular environment. The inner membranes of the endoplasmic reticulum (ER), Golgi apparatus, mitochondria and other membrane-bounded organelles of eukaryotic cells maintain the characteristic differences between the contents of each organelle and the cytosol (Alberts *et al.*, 1994).

All biological membranes have a common general structure, consisting of lipids, proteins and carbohydrates (Figure 1.2). The importance of membrane proteins is undeniable, if we consider that 30% of the eukaryotic genome is predicted to encode for membrane proteins (Engel and Gaub, 2008) and that membranes contain up to 80% w/w of proteins (Luckey, 2008). Channels, pores, pumps and transporters facilitate the exchange of impermeable molecules between cellular compartments and between the cells and their extracellular environment. Transmembrane receptors are also necessary for cellular responses to environmental signals, by sensing changes and initiating specific pathways. Moreover, they constitute more than 60% of approved drug targets and their structures are used for structure-based drug design (Yildirim *et al.*, 2007; Salom and Palczewski, 2011).

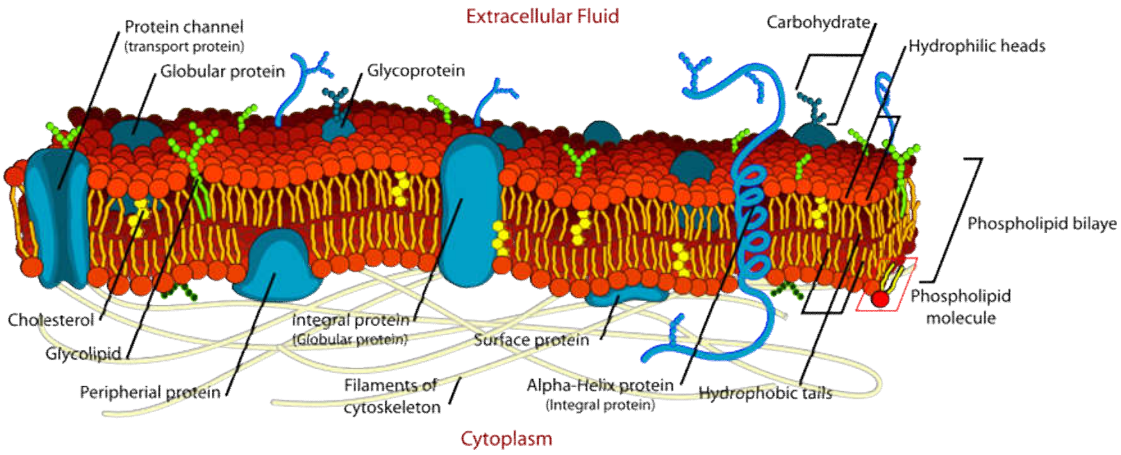

Figure 1.2. *Components of biological membranes (http://cellbiology.med.unsw.edu.au)*

The permeability properties of the membrane are determined by their lipid and protein components. In general, the lipid bilayer is penetrated by some small non-polar molecules but is nearly impermeable to ions and large or hydrophilic molecules (Figure 1.3). The movement of those molecules across the membrane is assisted by specialized membrane proteins or protein complexes.

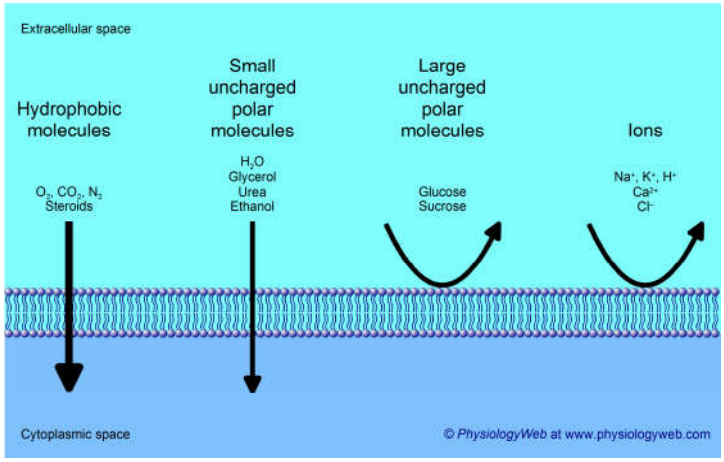

Figure 1.3. *Lipid bilayer permeability.*

We can distinguish a transport system to passive or active, depending on whether the transport is in the direction of or against electrochemical gradient respectively (Figure 1.4). Passive transport does not require energy consumption and may be through the lipid bilayer (simple diffusion), mediated by a channel (passive diffusion) or through a facilitator protein (facilitated diffusion).

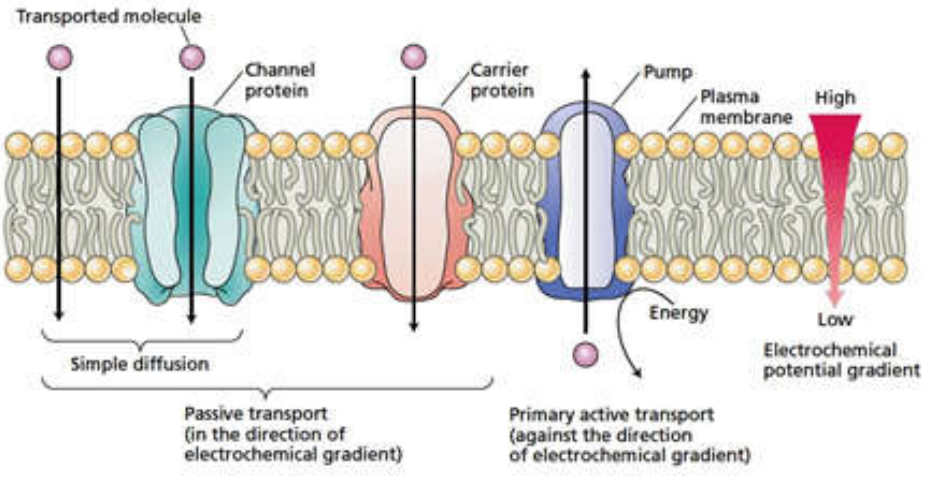

Figure 1.4. *Three classes of membrane transport proteins: channels, carriers, and pumps (source: Taiz L., Zeiger E., 2010).*

In contrast, active transport is energy-dependent and is mediated by transporters also called carriers or permeases. Primary active transport uses a primary source of energy such as adenosine-triphosphate (ATP) hydrolysis, light absorption or electron force. Secondary active transport uses electrochemical potentials of co-substrates as an energy source, by coupling the movement of the substrate against the electrochemical gradient to the movement of an ion, usually H^+ or Na^+, in the direction of the electrochemical gradient which is a releasing-energy procedure. Secondary active transporters can either be antiporters, which catalyze the exchange of one or more substances for another, or symporters, which transport two or more substances in the same direction (Figure 1.5). These transporters are present in many bacteria, fungi, plants and in higher eukaryotes with similar structure, consisting of a hydrophobic nucleus of 9-14 transmembrane domains with cytoplasmic hydrophilic N- and C-terminal regions. This structural model was a result of defining the relative hydrophobicity of amino acid residues in a protein sequence and was reinforced by biochemical, molecular and crystallographic results.

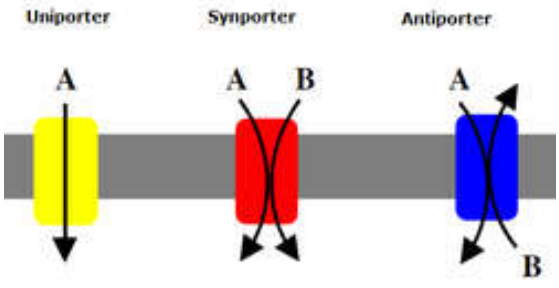

Figure 1.5. *Different types of transporters in active transport.*

Channel proteins do not need to bind the substrate, as they form hydrophilic pores that extend across the lipid bilayer allowing small molecules (usually ions) to

flow rapidly through them. On the other hand, carriers bind their substrate and undergo a series of conformational changes in order to transfer the solute across the membrane (Figure 1.6).

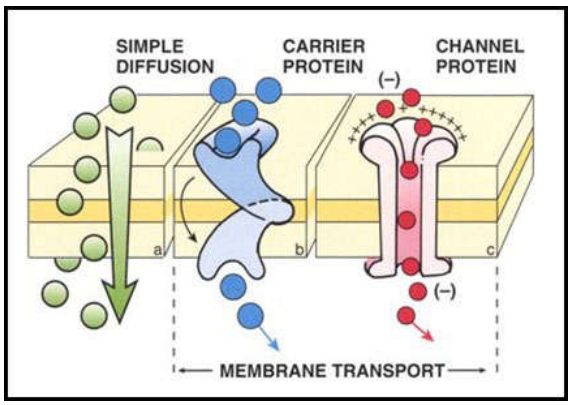

Figure 1.6. *Schematic depiction of carrier and channel proteins in membrane transport. (retrieved from: http://classes.kumc.edu/som/cellbiology/organelles/pm/tut4.html)*

1.3.2 Fungal nucleobase transporters - the NCS1/Fur family

Nucleobases (purines and pyrimidines) and their analogues are highly hydrophilic compounds that cannot diffuse across the lipid bilayer. Thus, their transport is mediated by specific transmembrane transporters which are present in many bacteria, fungi, algae, plants and mammals. They are very important not only in nucleotide and nucleic acid biosynthesis, but also in cell signaling, nutrition, response to stress and cell homeostasis (de Koning and Diallinas, 2000).

Genetic and biochemical studies established the presence of highly specific nucleobase transporters in fungi (Darlington and Scazzocchio, 1967), as they can use purines as good nitrogen sources but cannot grow in toxic concentrations of purines or pyrimidines caused either by an excess of a base (e.g. uric acid, uracil) or by a toxic analogue (e.g. oxypurinol, allopurinol, 8-azaguanine, 5-fluorouracil, 5-fluorocytosine, 5-fluorouridine) providing a powerful tool to select mutants and identifying the corresponding genes (Pantazopoulou and Diallinas, 2007; Galanopoulou *et al.,*2014).

Cloning and genome sequencing showed that the fungal nucleobase transporters belong to three evolutionary distinct protein families: the Nucleobase Cation Symporter family 1 (NCS1) also known as the Purine-Related Transporter family (PRT), the Nucleobase-Ascorbate Transporter family (NAT), also known as Nucleobase Cation Symporter family 2 (NCS2) and the AzgA-like family. All three families are classified as secondary active transporters, catalyzing the symport of purines with protons (De Koning and Diallinas, 2000; Pantazopoulou and Diallinas, 2007).

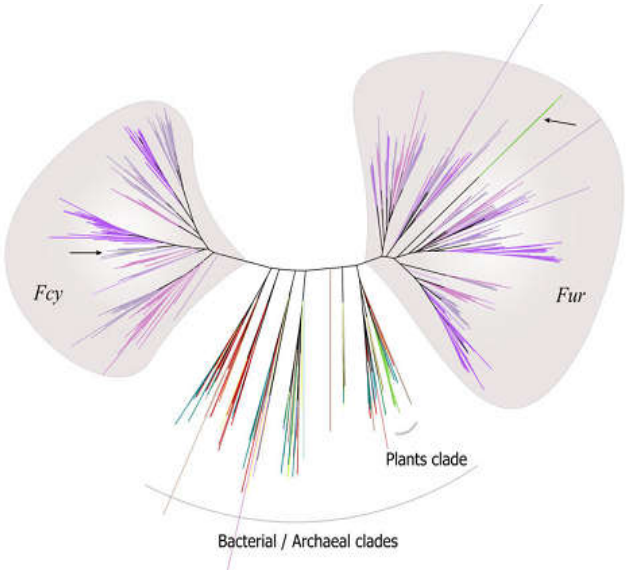

Figure 1.7. *Phylogenetic alalysis of NCS1 family (Krypotou et al. 2015b).*

Members of the NCS1 family are in general 419-635 amino acids long and most probably possess 12 putative transmembrane domains. N- and C-terminal regions are predicted to be cytoplasmic, while some of them have been shown to function as H^+ symporters. They are present in prokaryotes, fungi and some plants and they include transporters of purines, cytosine, uridine, allantoin, pyridoxine or thiamine (http://www.tcdb.org/browse.php). In 2008, crystal structure of a bacterial member of the NCS1 family named Mhp1 benzyl-hydantoin permease from *Microbacterium liquefaciens* was reported (Weyand *et al.,* 2008). Mhp1 contains 12 transmembrane α-helices, 10 of which are arranged in two inverted repeats of five helices, resulting in a topology very similar to that of LeuT.

Two members of NCS1 family have been characterized in *Saccharomyces cerevisiae*. The Fcy2p adenine-guanine-hypoxanthine-cytosine permease (Weber *et al.,* 1990) and the Fur4p uracil permease (Jund *et al.,* 1988) show limited overall sequence identity (19%) but show significant local similarity and share common motifs (De Koning and Diallinas, 2000). In *A. nidulans*, the NCS1 transporters are further classified in two sub-families based on their primary amino acid sequences and specificity profiles: the Fcy-like and the Fur-like transporters, as proved from phylogenetic alalysis (Figure 1.7) (De Koning and Diallinas, 2000; Pantazopoulou and Diallinas, 2007; Krypotou *et al.,* 2015b, Sioupouli *et al.,* 2017). A large number of NCS1 paralogues of unknown function is evident in most species, especially in fungi. For instance, *A. nidulans* has five Fcy-like and seven Fur-like proteins, but only three of them have a known major function; FcyB is a cytosine-purine transporter (Vlanti and Diallinas, 2008; Krypotou *et al.*, 2012), whereas FurA and FurD are allantoin and uracil transporters respectively (Amillis *et al.*, 2007; Hamari *et al.*, 2009). Null mutations of all other Fcy or Fur proteins do not lead to the apparent loss of any

detectable transport activity (Hamari *et al.*, 2009, Krypotou and Diallinas, 2014). All Fur transporters, except FurB, are localized in the plasma membrane. Among other *A. nidulans* Fur or Fcy proteins, some function as very minor permeases and some are cryptic transporters that are not expressed under standard laboratory conditions. In particular, FurE is a very low-affinity secondary allantoin transporter, also recognizing uracil, uric acid, 5-fluorocytosine and 5-fluorouridine when overexpressed, while FurC, FurF and FurG are minor uracil transporters and FurB is a putative 'proto-pseudogene' (Krypotou *et al.,* 2015b). Finally, FcyD and FcyE are cryptic transporters specific for adenine or guanine, both function detected solely upon overexpression (Sioupouli *et al.,* 2017). 1.3.3 Regulation of transporter endocytosis

Transmembrane proteins are often subject to tight regulation, allowing cells to adopt in different nutrient needs or stress conditions and protecting them from self-poisoning, especially when compounds such as heavy metals are essential for cell physiology but toxic when in excess. Such a control occurs at the level of protein trafficking –including secretion toward the plasma membrane (PM), direct vacuolar sorting, endocytosis, endosomal recycling and turnover in the vacuole/lysosome. The major regulatory mechanism is ubiquitilation, an evolutionary conserved process from fungi to mammal (Durpé *et al.,* 2004; Miranda and Sorkin, 2007; Lauwers et al., 2010).

Protein ubiquitination is a post-translational conjugation of ubiquitin to a target protein, by the formation of an isopeptide bond between the C-terminal glycine of ubiquitin and the amino group of a lysine residue in the target protein. Ubiquitin is a 76-amino acid protein, highly conserved and present in all eukaryotic organisms and cell types. In *S. cerevisiae* the ubiquitination of transporters is exclusively carried out by the HECT (homologous to E6-AP carboxyl-terminus) ubiquitin ligase Rsp5, which is the only member of the Nedd (neural precursor cell expressed developmentally downregulated) 4/Nedd4-like family of ubiquitin ligases in yeast. *A. nidulans* has a single orthologue of Rsp5, called HulA (HECT ubiquitin ligase).

1.3.4 Principal goals of this work

The main target of this dissertation was to study the structural, functional or regulatory role of the C-terminal region of NCS1-Fur transporters. For this, we used three Fur transporters, namely FurA, FurD and FurE, which in addition to their distinct transport activities, also show differential sensitivities to endocytic turnover rates. We first provided evidence showing that the C-terminal region is critical for endocytic down regulation through HulA-dependent ubiquitination. Importantly and somehow surprisingly, we further found that the cytoplasmically located N- and C-terminal segments of FurE interact with each other and this interaction is critical for

the proper functioning of external and internal gates, and thus important for substrate specificity. Our results are discussed under the light of available knowledge coming from crystallographic and *in silico* approaches of homologous transporters.

2. Materials and Methods

2.1 Strains used in this study

The strains used in this study are included in Table 2.1 (*see* next page).

2.2 Culture media and growth conditions

Aspergillus nidulans

Two different types of media were used for the growth of fungal cultures, the complete medium and the minimal medium. The complete medium contained all the elements required for fungal growth, thus enabling all strains to grow normally and independently of their auxotrophies. The minimal medium contained the minimum nutrients for fungal growth. That is salt solution, carbon source (glucose, fructose or sucrose), nitrogen source and the appropriate auxotrophies, according to the requirements of each strain. Composition of all media and the solutions used are shown in Table 2.2 and Table 2.3 respectively. Depending on the purpose of the culture, growth media were used in a liquid or a solid form. For the latter, 1-2% agar was added before autoclaving.

Table 2.2 Composition of culture media for the growth of *A. nidulans* (Cove 1966; Scazzocchio *et al*., 1982).

	Complete Medium (CM)	**Minimal Medium (MM)**	**Sucrose Minimal Medium (SM)**
H_2O_{dist}	1 L	1 L	1 L
Salt solution	20 mL	20 mL	20 mL
Vitamine solution	10 mL	-	-
D-Glucose/D-Fructose	10 g	10 g/1 g	10 g
Casamino acids	1 g	-	-
Bactopeptone	2 g	-	-
Yeast extract	1 g	-	-
Sucrose	-	-	342.3 g

Table 2.3 Solutions used in A. nidulans culture media of Table 2.2.

Salt solution		**Vitamine solution**		**Trace elements***	
H_2O_{dist}	1 L	H_2O_{dist}	1 L	$Na_2B_4O_7$ x $10H_2O$	40 mg
KCl	26 g	p-aminobenzoic acid	20 mg	$CuSO_4$ x $5H_2O$	400 mg
$MgSO_4$ $7H_2O$	26 g	biotin	1 mg	FeO_4P x $4H_2O$	714 mg
KH_2PO_4	76 g	D-pantothenic acid	50 mg	$MnSO_4$ x $1H_2O$	728 mg
Chloroform	2 mL	riboflavin	50 mg	Na_2MoO_4 x $2H_2O$	800 mg
Trace elements*	50 mL	pyridoxine	50 mg	$ZnSO_4$ x $7H_2O$	8 mg

Table 2.1. Strains used in this study.

Strain Genotype	References
ΔuapA UapC::pyrG ΔazgA ΔFcyB::argB ΔFurD::riboB ΔFurA::riboB ΔcntA pabaA1 pantoB100	Krypotou and Diallinas, 2014
ΔuapA UapC::pyrG ΔazgA ΔFcyB::argB ΔFurD::riboB ΔFurA::riboB ΔcntA pabaA1 pantoB100 pGEM-gpdAp-FurA GFP pantoB	Krypotou *et al.*, 2015
ΔuapA UapC::pyrG ΔazgA ΔFcyB::argB ΔFurD::riboB ΔFurA::riboB ΔcntA pabaA1 pantoB100 pGEM-gpdAp-FurD-GFP pantoB 4	Krypotou *et al.*, 2015
ΔuapA UapC::pyrG ΔazgA ΔFcyB::argB ΔFurD::riboB ΔFurA::riboB ΔcntA pabaA1 pantoB100 pGEM-gpdAp-FurE-GFP pantoB 8	Krypotou *et al.*, 2015
ANID_01089.1Δ::AFpyrG nkuAΔ::argB riboB2 pyroA4 pyrG89	Karachaliou *et al.*, 2013
ANID_09105.1Δ::AFriboB nkuAΔ::argB pyrG89 pyroA4 riboB2	Karachaliou *et al.*, 2013
ΔuapA UapC::pyrG ΔazgA ΔFcyB::argB ΔFurD::riboB ΔFurA::riboB ΔcntA pabaA1 pantoB100 pGEM-gpdAp-FurE-K252F pantoB	Krypotou *et al.,* 2015
uapAΔ uapCΔ::AFpyrG azgAΔ fcyBΔ::argB furDΔ::AFriboB furAΔ::AFriboB cntAΔ::AFriboB pantoB100 pabaA1 pGEM-gpdAp-FurD-K531Δ-GFP-trpC-pantoB	this study
uapAΔ uapCΔ::AFpyrG azgAΔ fcyBΔ::argB furDΔ::AFriboB furAΔ::AFriboB cntAΔ::AFriboB pantoB100 pabaA1 pGEM-gpdAp-FurA-K534Δ-GFP-trpC-pantoB	this study
uapAΔ uapCΔ::AFpyrG azgAΔ fcyBΔ::argB furDΔ::AFriboB furAΔ::AFriboB cntAΔ::AFriboB pantoB100 pabaA1 pGEM-gpdAp-FurE-K498Δ-GFP-trpC-pantoB	this study
uapAΔ uapCΔ::AFpyrG azgAΔ fcyBΔ::argB furDΔ::AFriboB furAΔ::AFriboB cntAΔ::AFriboB pantoB100 pabaA1 artBΔ::AFpyrG pGEM-gpdA-FurA-GFP-trpC-pantoB	this study
uapAΔ uapCΔ::AFpyrG azgAΔ fcyBΔ::argB furDΔ::AFriboB furAΔ::AFriboB cntAΔ::AFriboB pantoB100 pabaA1 artBΔ::AFpyrG pGEM-gpdA-FurA-GFP-trpC-pantoB	this study
uapAΔ uapCΔ::AFpyrG azgAΔ fcyBΔ::argB furDΔ::AFriboB furAΔ::AFriboB cntAΔ::AFriboB pantoB100 pabaA1 pGEM-gpdAp-FurA-K551R-GFP-trpC-pantoB	this study
uapAΔ uapCΔ::AFpyrG azgAΔ fcyBΔ::argB furDΔ::AFriboB furAΔ::AFriboB cntAΔ::AFriboB pantoB100 pabaA1 pGEM-gpdAp-FurD-K531R-GFP-trpC-pantoB	this study
uapAΔ uapCΔ::AFpyrG azgAΔ fcyBΔ::argB furDΔ::AFriboB furAΔ::AFriboB cntAΔ::AFriboB pantoB100 pabaA1 pGEM-gpdAp-FurD-K537/539R-GFP-trpC-pantoB	this study
uapAΔ uapCΔ::AFpyrG azgAΔ fcyBΔ::argB furDΔ::AFriboB furAΔ::AFriboB cntAΔ::AFriboB pantoB100 pabaA1 pGEM-gpdAp-FurE-K521/522R-GFP-trpC-pantoB	this study
uapAΔ uapCΔ::AFpyrG azgAΔ fcyBΔ::argB furDΔ::AFriboB furAΔ::AFriboB cntAΔ::AFriboB pantoB100 pabaA1 pGEM-gpdAp-FurC-E-GFP-trpC-pantoB	this study
uapAΔ uapCΔ::AFpyrG azgAΔ fcyBΔ::argB furDΔ::AFriboB furAΔ::AFriboB cntAΔ::AFriboB pantoB100 pabaA1 pGEM-gpdAp-FurD KKK-GFP-trpC-pantoB	this study
uapAΔ uapCΔ::AFpyrG azgAΔ fcyBΔ::argB furDΔ::AFriboB furAΔ::AFriboB cntAΔ::AFriboB pantoB100 pabaA1 pGEM-gpdAp-FurE-ΔC509-GFP-trpC-pantoB	this study
uapAΔ uapCΔ::AFpyrG azgAΔ fcyBΔ::argB furDΔ::AFriboB furAΔ::AFriboB cntAΔ::AFriboB pantoB100 pabaA1 pGEM-gpdAp-FurE K252F-K498-GFP-trpC-pantoB	this study
uapAΔ uapCΔ::AFpyrG azgAΔ fcyBΔ::argB furDΔ::AFriboB furAΔ::AFriboB cntAΔ::AFriboB pantoB100 pabaA1 pGEM-gpdAp-FurE ΔN21-GFP-trpC-pantoB	this study
uapAΔ uapCΔ::AFpyrG azgAΔ fcyBΔ::argB furDΔ::AFriboB furAΔ::AFriboB cntAΔ::AFriboB pantoB100 pabaA1 pGEM-gpdAp-FurE ΔN38-GFP-trpC-pantoB	this study

The adjustment of pH at 6.8 was achieved with the use of NaOH 3N. The final concentration of nitrogen sources was 10mM for $NaNO_3$, 10mM for Ammonium L-(+)-tartrate and 5mM for urea. Purines were used at 0.1 mg/mL, amino acids at 5mM, 8-Aza-guanine at 0.2-0.4 mM in the presence of $NaNO_3$ as sole nitrogen source, uracil at 5 mM and uridine at 10 mM. The toxic analogues 5-fluorocytosine, 5-fluorouracil and 5-fluorouridine were used at 50 μM, 100 μM and 10 μM respectively.

The cultures were inoculated with conidiospores harvested from sporulating culture plates by using sterile toothpicks or the inoculation loop. Solid cultures were incubated in 37^{o}C or 25 ^{o}C for 2-5 days and liquid cultures were incubated in 37 ^{o}C or 25 ^{o}C at 140 rpm.

Derepression of proteins expressed under a strong ethanol-inducible, glucose-repressible alcohol dehydrogenase (*alc*A) promoter was achieved by the use of 0.1% w/v fructose as a sole carbon source, while their induction was achieved by addition of 0.4% v/v ethanol in derepressing media.

Escherichia coli

Luria-Bertani media (LB Lennox: BactoTryptone 10 g/L, NaCl 5 g/L, BactoYeast Extract 5 g/L) and pH 7.0 was used for the growth of bacterial cultures (Sambrook *et al.*, 1989), in liquid or solid form (1% w/v agar added). For the selection of transformed colonies, ampicillin in final concentration 100 μg/mL was added. Solid bacterial cultures were incubated overnight at 37^{o}C and liquid cultures were additionally agitated at 200 rpm.

2.3 Storage conditions of *Aspergillus nidulans*

For long-term storage, fungi strains can be preserved in glycerol stocks, in which conidiospores from a fresh CM plate were harvested in 700 μL PBS buffer (Table 2.4) in a sterile eppendorf tube and 700 μL of glycerol was added. After vortexing, the glycerol tubes were stored at -80^{o}C.

Table 2.4 Composition of PBS buffer.

	Concentration (g/L)
NaCl	8.0
KCl	0.2
Na_2PO_4	1.44
KH_2PO_4	0.24

2.4 Genetic crosses and progeny analysis in *Aspergillus nidulans*

Multiple mutant strains for genetic analysis can be constructed by meiotic crossing (Todd *et al.*, 2007). *Aspergillus nidulans* is homothallic, which means than it is self-fertile, but crosses can be initiated by hyphal fusions between homokaryons with genetically different nuclei. The resulting heterokaryons can be forced to maintain a balanced ratio of the component nuclei by including complementing auxotrophic

mutations in the parental nuclei and forcing growth without the corresponding supplements (Casselton and Zolan, 2002). The result of a karyogamic event is the formation of cleistothecia. In order to obtain strains with a desired genotype, the following experimental procedure was performed.

Preparation

Two different parental strains of interest were inoculated in pairs, with a distance of 1-2 cm between them, in minimal media with the appropriate vitamine supplements. The cultures were incubated in 37^{O}C for 2 days. Small parts of media in the contact area of the two parental strains mycelia were removed with a sterile toothpick and transferred in small Petri dishes, containing nitrate as nitrogen source and only the supplements required from both parental strains. Therefore, only heterokaryons were able to produce the missing supplements and grow on the plates. After 1-2 days of incubation at 37^{O}C, the plates were sealed with adhesive tape and incubated for further 14-20 days at 37^{O}C, in order to form cleistothecia.

Selection of cleistothecia

The plates were unsealed and 8 single cleistothecia were selected with a sterile toothpick. Surrounding cells and media were removed by rolling cleistothecia on an agar plate. Finally, each cleistothecium was burst open by mechanical forces and the ascospores were released in an eppendorf tube containing 500 μL of sterile water. An aliquot (~10 μL) of each ascospore suspension was plated on minimal media selecting against both parental types and was incubated at 37^{O}C for 3 days, so that only recombinant progeny would grow. Different dilutions of the suspension from one recombinant cleistothecium were plated In order to obtain single colonies, which were then selected and analyzed for their genetic background.

Progeny analysis

For the characterization of unknown strains in *Aspergillus nidulans*, growth tests are performed, comparing their growth with that of well-studied control strains in different conditions of temperature, pH, nitrogen or carbon sources, supplements, toxic analogues and antibiotics. Replica plates with the appropriate media were used in pursuit of distinct phenotypes. Further genetic analysis is usually required for their complete genetic characterization by the use of polymerase chain reaction (PCR) or epifluorescence microscopy.

2.5 Epifluorescence microscopy

Samples for inverted fluorescence microscopy were prepared as previously described (Valdez-Taubas *et al.,* 2004; Gournas *et al*., 2010; Karachaliou *et al.*, 2013). In particular, sterile 35 mm l-dishes with glass bottom (Ibidi, Germany) containing

liquid minimal media supplemented with $NaNO_3$ and 0.1% glucose (for experiments with the strong *gpdAp* promoter) or fructose (for experiments with the *alcAp* promoter) were inoculated from a spore solution and incubated for 16-22 hours at 25^{o}C. For the observation of proteins expressed by the *alcAp* promoter, 0.4% v/v ethanol in derepressing media for 2 hours or overnight was added in order to achieve full induction of expression.

The samples were observed on an Axioplan Zeiss phase contrast epifluorescent microscope and the resulting images were acquired with a Zeiss-MRC5 digital camera using the AxioVs40 V4.40.0 software. Image processing, contrast adjustment and color combining were made using Adobe Photoshop CS3 software or ImageJ software.

Quantification

For quantifying transporters endocytosis, Vacuolar Surface (Total surface of vacuoles containing GFP/hypha) and Vacuolar GFP Fluorescence (Total fluorescence intensity of vacuoles containing GFP/hypha) were measured using the Area Selection Tool of ICY application. Turkey's Multiple Comparison Test (One-Way ANOVA) was performed to test the statistical significance of the results for 5 Regions of Interest (ROIs), using Graphpad Prism 3. Images were further processed and annotated in Adobe Photoshop CS3.

2.6 DNA manipulations

2.6.1 Preparation of genomic DNA from Aspergillus nidulans

The protocol used for the extraction of 10-20 μg of genomic DNA is based on the protocol described in Lockington *et al.* (1985). Complete medium culture plates were incubated for 4 days at 37^{o}C. Conidiospores from ¼ of a plate were harvested in 25 mL of minimal media containing NH_4^+ as nitrogen source and all the supplements required (depending on the auxotrophies carried by the strains used). Liquid cultures were incubated overnight at 37^{o}C, 140 rpm. The next day, the culture was filtered through a blutex, squeezed between two papers to remove excessive liquid and immediately frozen in liquid nitrogen. The mycelia were pulverized in a mortar with a pestle in the presence of liquid nitrogen and ~200 mg of the fine powder were transferred in a 2mL eppendorf tube. The mycelia powder was resuspended in 800 μL of DNA extraction buffer (0.2 M Tris-HCl pH 8.0, 1% SDS, 1 mM EDTA pH 8.0), mixed by vortexing and incubated on ice for 5-20 min. Then, 800 μL of phenol were added and the mixture was shaken vigorously and centrifuged for 5 min at 12000 rpm. The upper phase containing the DNA was transferred to a new 2mL eppendorf tube, equal volume of chloroform was added and the mixture was shaken vigorously and centrifuged for 5 min at 12000 rpm. The upper phase was transferred again, to a new 2mL eppendorf tube where DNA was precipitated by adding equal volume of

isopropanol and 1/10 volume of 3M CH_3COONa pH 5.3. The mixture was gently mixed by inverting the tube several times and was then centrifuged for 10 min at 12000 rpm. The pellet was washed with 200 μL 70% ethanol without mixing and after a 2 min centrifusion at 12000 rpm ethanol was removed with a pipette. The pellet was dried for 5-10 min at 50^{o}C, resuspended in 100 μL of sterile distilled water containing 0.2 mg/mL RNaseA and incubated at 37^{o}C for 30 min. In order to analyze the quantity and quality of the extracted DNA, agarose gel electrophoresis was performed to an aliquot (2 μL) of the DNA solution.

2.6.2 Restriction Endonuclease Digestion

Restriction endonucleases are enzymes found in archaea and bacteria and their physiological role is to provide a defense mechanism against invading viruses. They cleave DNA at specific target sequences called *restriction sites*, which are mostly palindromic. DNA was digested with restriction endonucleases in order to yield specific DNA fragments for downstream manipulations. More specifically, the appropriate amount of DNA was incubated with 1 μL restriction enzyme, 1x restriction enzyme buffer and distilled water to reach the final volume of the reaction at the optimal temperature of the enzyme for 1.30-2 hours or overnight. Digested DNA was then analyzed by agarose gel electrophoresis.

2.6.3 Agarose gel electrophoresis

Agarose gel electrophoresis was used for the analysis of size and conformation of DNA in a sample, quantification of DNA and the separation and extraction of DNA fragments. 0,8% or 1.2% agarose was dissolved in 1x TAE buffer (242 g Tris-Base, 57.1 mL glacial CH_3COOH, 100 mL 0.5 M EDTA pH 8.0 for 1L 50x buffer) by warming up the solution in the microwave. After cooling down to 70^{o}C, 0.5 mg/mL ethidium bromide (EthBr) was added and the solution was poured into a casting tray and left to harden. The DNA samples were mixed with loading buffer and then loaded to the gel. A molecular weight marker was loaded along with the samples, in order to determine the size of the fragments. Gels were run at 100 V, exposed to UV light with a UV transilluminator and DNA bands were visualized and photographed due to the intercalating fluorescent dye (EthBr).

2.7 Polymerase Chain Reaction (PCR)

2.7.1 Standard PCR reactions

Conventional PCR reactions were performed using KAPATaq DNA polymerase (Kapa Biosystems). Provided that the amplified fragment would be used for molecular cloning or transformation a high fidelity KAPA HiFi HotStart Ready Mix

(Kapa Biosystems) polymerase was used in order to lower error frequency. Components and conditions of these PCR reactions are described in the Tables 2.5 and 2.6, according to manufacturer instructions.

Table 2.5 Composition of conventional and high fidelity PCR reactions.

Components	**Final Concentration**	
	Conventional	High Fidelity
10x polymerase buffer*	1x	-
dNTPs	200 μM of each	-
2x Polymerase Ready mix	-	1x
Forward primer	0.4 μM	0.4 μM
Reverse primer	0.4 μM	0.4 μM
DNA polymerase	KapaTaq 1 μL	-
DNA template	10-20 ng	10 ng
H_2O_{dist}	up to 25 μL	up to 25 μL

*with 1.5 mM $MgCl_2$

Table 2.6 Conditions used for conventional, high fidelity and site-directed mutagenesis PCR reactions.

Steps	Conventional		High Fidelity		Mutagenesis	
	^oC	Duration	^oC	Duration	^oC	Duration
1	95	5 min	95	3 min	95	3 min
2	95	30 sec	98	20 sec	98	30 sec
3	T_m*-5	30 sec	60-75	15 sec	60-75	1 min
4	72	1 min/kb	72	15-16 sec/kb	72	5 min
5	steps 2-4	x25 cycles	steps 2-4	X30 cycles	steps 2-4	x18 cycles
6	72	10 min	72	10 min	72	10 min
7	12	∞	12	∞	12	∞

*The formula used for estimating the T_m of the primers is: T_m=69.3+0.41(%GC)-650/L-(%mismatch)

2.7.2 In vitro site-directed PCR mutagenesis

For site-directed mutagenesis, a pair of complimentary primers was designed for each mutation. The primers were long (35-40 nucleotides) with >50% GC-content and the mutation was located in the middle of the sequence, so that annealing to the complementary sequence of the template DNA would not be severely affected by the mismatch. Codon substitutions were designed in a way that the least possible number of mismatches would occur, by taking advantage of the redundancy of the genetic code, while the resulting codons would be frequently encountered in *A. nidulans* genome. Furthermore, designed mutations, if possible, led to the introduction of a restriction site that would enable direct diagnostic digestion after mutagenesis. High fidelity PCR reactions for *in vitro* site-directed PCR mutagenesis

were carried out using KAPA HiFi HotStart Ready Mix (Kapa Biosystems) polymerase. Components and conditions for this type of PCR are described in Tables 2.5 and 2.6.

After amplification, the PCR product was incubated at 37^{o}C for 2 h with 1 μL of the restriction enzyme *Dpn*I (TaKaRa), which cleaves methylated (GA^{m}|TC) DNA strands so that parental non-mutated plasmids were fragmented. The resulting solution was used to transform *E. coli* competent cells. Plasmid DNA from the ampicillin-resistant colonies was prepared, diagnostic digestion with the appropriate restriction endonucleases was performed and the sample was sent for sequencing. Finally, plasmids with the desired mutation were transformed in *A. nidulans.*

2.8 Molecular cloning

This experimental procedure includes the cleavage of circular plasmid DNA with one or more restriction endonucleases, its ligation *in vitro* to foreign DNA fragment bearing compatible termini, transformation of *E. coli* with the products of the ligation reaction and screening of the transformed, ampicillin-resistant colonies for those carrying the desired DNA sequences. This method takes advantage of the fact that a single bacterial cell can be induced to take up and replicate a single recombinant DNA molecule (Sambrook and Russel, 2001).

2.8.1 Preparation of cloning vector and insert

The first step of molecular cloning is the preparation of the cloning vector and the DNA fragment of interest (hereafter referred to as "insert"). In particular, the insert was amplified by PCR using primers that added the desired restriction sites to its termini and was subsequently digested with the corresponding restriction endonucleases. A cloning vector that contained recognition sequences for the same restriction enzymes in its multiple cloning site was selected and subjected to digestion in order to generate sticky ends complementary to those of the digested insert (Sambrook and Russel, 2001). The digested vector and the insert were purified from agarose gel using the Nucleospin Extract II Kit (Macherey-Nagel). The corresponding DNA bands were quickly excised from the gel under low-strength UV light exposure to avoid DNA damage, transferred into an eppendorf tube and processed as described in the manufacturer instructions.

In cases where the termini of the resulting linearized plasmid were complementary (e.g. when cloning with one restriction enzyme), the digested vector was incubated at 37^{o}C for 15 min with 1 μL of calf intestine alkaline phosphatase CIAP (TaKaRa) before being loaded to the agarose gel. Removal of the 5'-terminal phosphate groups is necessary in order to avoid self-ligation of the linearized vector and also improved ligation efficiency by diminishing the background of transformed bacterial colonies that carry "empty" vectors (Sambrook and Russel, 2001).

2.8.2 Generation of recombinant DNA

Generation of recombinant DNA was mediated by DNA ligase, an enzyme that covalently links the complementary sticky ends together. The purified vector and insert were mixed at a 1:3 concentration ratio along with 1 μL of T4 DNA ligase (TaKaRa) and 1x ligase buffer in 10 μL total volume. The reaction was incubated at 25^{o}C for 1.5 h and was then used to transform *E. coli* competent cells.

2.8.3 Introduction of recombinant DNA into E. coli

Preparation of competent cells

A trace of DH5a *E. coli* cells from the glycerol stock was streaked on an LB agar plate and was incubated at 37^{o}C overnight. 5 mL LB medium were inoculated with a single colony from the plate and were incubated for 16 h at 37^{o}C, 200 rpm. An aliquot of 0.5 mL of the saturated culture was used to inoculate 400 mL LB medium in a 1 L conical flask and was incubated at 37^{o}C, 260 rpm until an OD_{600} of 0.45-0.55 had been reached. The culture was then centrifuged at low speed (4.500 g), at 4^{o}C for 5 min and the supernatant was discarded. The cell pellet was gently resuspended in 0.4x original volume of ice-cold transformation buffer I (30 mM CH_3COOK, 10 mM $CaCl_2$, 50 mM $MnCl_2$, 100 mM $RbCl_2$, 15% glycerol, pH 5.8 with 1 M CH_3COOH) and incubated on ice for an additional 5 min. The cells were collected by centrifugation at 4500 g, 4^{o}C for 5 min and were resuspended carefully in 1⁄25 original volume of ice-cold transformation buffer II (10 mM MOPS pH6.5, 75 mM $CaCl_2$, 10 mM $RbCl_2$, 15% glycerol, pH 6.5 with 1 M KOH). The cells were again incubated on ice for 15-60 min and aliquots of 200 μL were distributed in sterile 1.5 mL eppendorf tubes and frozen in liquid nitrogen. The competent cells were then stored at -80^{o}C.

E. coli transformation

About 0.01-0.5 μg of plasmid DNA was added in 200 μL of defrosted *E. coli* competent cells, mixed and incubated on ice for 30 min. The cells were then subjected to heat shock by incubation at 42^{o}C for 90 sec in a heat block and immediate moving of the tube on ice for another 2 min. To allow expression of the ampicillin resistance gene of the plasmid, 1 mL of liquid LB medium was added and the cells were incubated at 37^{o}C for 1 h. The cells were harvested by quick spin at 13.000 rpm for 30 sec, they were resuspended in ~100 μL of LB medium and spread on LB agar plates containing ampicillin at a final concentration of 100 μg/mL. The plate was incubated at 37^{o}C overnight.

Preparation of plasmid DNA from E. coli

For high purity plasmid DNA preparation, the (Macherey-Nagel) Nucleospin Plasmid Kit was used. In cases that no high purity was required, an adaptation of the protocol described in Sambrook and Russel (2001) was used. In particular, 5 mL of LB medium with ampicillin were inoculated with a single bacterial colony carrying the desired plasmid and were incubated overnight at 37^{o}C, 200 rpm. 1-1.5 mL of the bacterial culture was centrifuged at 12000 rpm for 1 min and the pellet was resuspended in 200 μL of cell suspension buffer (50 mM Tris-HCl pH 8.0, 10 mM EDTA) by vortexing. Then, 200 μL of cell lysis solution (200 mM NaOH, 1% SDS) were then added and mixed by inverting the tube, followed by 200 μL neutralization buffer (3 M CH_3COONa pH 5.5). The cell suspension centrifuged at 12000 rpm for 5 min and the supernatant was collected in a new eppendorf tube. 500 μL of isopropanol were added and the sample was mixed and centrifuged at 12000 rpm for 5 min to precipitate the DNA. The DNA was washed with 70% v/v ethanol to remove co-precipitated salt and to replace the isopropanol with the more volatile ethanol, thus making DNA easier to redissolve. The pellet was dried for 5 min at 50^{o}C and was resuspended in 100 μL of sterile distilled water with 0.2 mg/mL RNase. An aliquot was used for diagnostic digestions or PCR that would confirm the successful cloning of the desired DNA sequence, as well as the orientation of insertion.

2.8.4 Aspergillus nidulans DNA transformation

Aspergillus nidulans transformation was performed as described in Koukaki *et al.* (2003). In particular, conidiospores were harvested from a full grown CM culture plate and filtered through blutex. 200 mL minimal media (in a 1 L conical flask) with the appropriate supplements and nitrogen source were inoculated with the spore solution and were incubated at 37^{o}C for 4-4.45 h, 140 rpm. After 3.5 h of incubation, an aliquot of the culture was regularly observed under the microscope for the appearance of germ tubes. Once conidia were at the germinative phase, incubation was stopped and the culture was transferred into sterile falcons and centrifuged at 4000 rpm for 10 min. The pellet was resuspended in 20 mL of Solution I (1.2 M $MgSO_4$, 10 mM orthophosphate pH 5.8) and was poured into a sterile 250 mL conical flask. About 200 mg of the lytic enzyme glucanex, together with a few crystals of Bovine Serum Albumin (BSA) were then added for the disruption of the cell wall and release of the protoplasts. The spore suspension was incubated for 5 min on ice and then for 1.5-2 h at 30^{o}C, 60 rpm. Protoplasts were concentrated by centrifugation at 4000 rpm for 10 min and washed with 10 mL Solution II (1 M sorbitol, 10 mM Tris-HCl pH 7.5, 10 mM $CaCl_2$). The pellet was then resuspended in Solution II at a volume depending on the number of transformations desired. Protoplasts were distributed in eppendorf tubes and plasmid DNA was added in final concentration of 1.5-2 μg

followed by ¼ of the total volume Solution III (60% w/v PEG6000, 10 mM Tris-HCl pH 7.5, 10 mM $CaCl_2$). A control tube without DNA was included in order to evaluate whether the protoplasts and the solutions used were free of contaminations. Tubes were incubated on ice for 15 min and 500 µL of Solution III were added, mixed and incubated for another 15 min at room temperature (RT). The tubes were then centrifuged at 6000 rpm for 10 min, protoplasts were washed with 1 mL of Solution II and resuspended in 200 µL of the latter. Protoplasts were transferred into 15 mL sterile falcons containing 4 mL of melted Top Sucrose Minimal Media (0.45% agar, 20 mL salt solution, 10 g D-glucose, 342,4 g sucrose for 1 L), carefully mixed and quickly used to inoculate previously prepared SM (sucrose minimal media; 1% agar). Plates were incubated at 37^{o}C for 4-5 days and transformants were isolated by streaking on minimal media and analyzed by growth tests.

2.9 Kinetic analysis of transporters

Kinetic analysis of Fur transporters activity was measured by estimating uptake rates of [^{3}H]-uracil uptake, as previously described in Koukaki *et al.* (2005) and Papageorgiou *et al.* (2008). Briefly, conidiospores from a fresh CM culture plate were harvested in 25 mL of minimal media containing nitrate and all the necessary supplements, filtered through a blutex and incubated at 37^{o}C, 140 rpm for 4 h.

In *Aspergillus nidulans*, [^{3}H]-uracil uptake was assayed at 37^{o}C in germinating conidiospores, just prior of germ tube emergence. The culture was centrifuged for 10 min at 4000 rpm and conidiospores were resuspended in minimal media without nitrogen source and supplements, at final concentration 10^{7} conidiospores/µL. The resulting spore solution was distributed in 1.5 mL eppendorf tubes (75 µL in each tube) and these were equilibrated for 10 min at 37^{o}C in the heat block. Initial velocities were measured at 1 min and at 4 min of incubation with 25 µL of radioactive substrate for FurD and FurE respectively. Reactions were terminated by adding 1000-fold excess of ice-cold non-radiolabelled substrate. To remove non-incorporated radioactivity, the spore suspension was washed with ice-cold minimal media (12500 rpm, 5 min). The supernatant was removed by sunction and the pellet was finally resuspended in 1 mL of scintillation solution (666 mL toluol, 2.66 g PPO, 0.066 g POPOP, 333 mL Triton-X-100). The eppendorf tubes were inserted in scintillation vials and radioactivity was measured in a scintillation counter.

Initial velocities were corrected by subtracting background uptake values obtained in the simultaneous presence of 1000-fold excess of non-radiolabelled substrate. The background uptake level did not exceed 15-20% of the total counts obtained in wild-type strains. The K_m (concentration for obtaining V_m/2) of Fur transporters for uracil was obtained directly by performing and analyzing (Prism3) uptakes at various concentrations. All experiments were carried out in triplets.

2.10 Protein manipulations

2.10.1 Protein extraction from Aspergillus nidulans

Complete medium culture plates were incubated for 4 days at 37^{o}C. Conidiospores from a full plate were harvested in 100 mL of minimal media containing nitrate as nitrogen source and any supplements required. The liquid cultures were incubated for 14-16 h at 25^{o}C and then, they were filtered through blutex, squeezed between two papers to remove excessive liquid and immediately frozen in liquid nitrogen. The mycelia were pulverized 5-6 times in a mortar with a pestle in the presence of liquid nitrogen, and ~400 mg of the fine powder were collected in a 2 mL eppendorf tube.

Total protein extraction

The mycelia powder was resuspended in 1 mL of ice cold precipitation buffer (see Table 2.7), mixed by vortexing and incubated on ice for 10-30 min. The sample was then centrifuged for 5 min at 13000 rpm, 4^{o}C. The pellet was resuspended twice in ice cold acetone and the sample was centrifuged for 5 min at 13000 rpm, 4^{o}C. The supernatant was discarded and the pellet was incubated at 60^{o}C in a heat block, until it whitened and cracks appeared. The pellet was then resuspended in 500-600 µL of protein extraction buffer I and the sample was centrifuged for 10-15 min at 13000 rpm, 4^{o}C. The supernatant was transferred in a pre-frozen eppendorf tube and was stored at -80^{o}C for further use. Protein levels of the samples were quantified and normalized, before loading in gel electrophoresis. The samples were incubated with 4x sample buffer for 30 min at 37^{o}C (for membrane proteins).

Table 2.7 Solutions used for total protein extraction.

Solutions	Composition in H_2O_{dist}
Precipitation Buffer	50 mM Tris-HCl pH 8.0, 50 mM NaCl, 12.5% (v/v) trichloroacetic acis (TCA), 1 mM PMSF, 1x Protease Inhibitors Cocktail (PIC)
Extraction Buffer I	100 mM Tris-HCl pH 8.0, 50 mM NaCl, 1% (v/v) SDS, 1 mM EDTA, 1 mM PMSF, 1x PIC
4x sample loading buffer	40% (v/v) glycerol, 250 mM Tris-Hcl pH 6.8, 0.02% (w/v) bromophonol blue, 8% (v/v) SDS, 20% (v/v) β-mercaptoethanol

2.10.2 Protein quantification

The determinaton of protein concentration in the samples was done using the Bradford method (Bradford, 1976). The protein-dye complex causes a shift in the dye absorption maximum from 465 nm to 595 nm. The amount of absorption produced is proportional to the protein concentration. 1 mL Bradford Reagent (100 mg Coomassie Brillant Blue G-250, 50 mL 100% EtOH, 100 mL H_3PO_4, 850 mL H_2O) were

transferred in a cuvette and 2 µL of the protein sample were added and vertexed briefly. Prior to reading the absorbance, 1 mL of this reagent was used to calibrate the spectrophotometer. The optical density (OD) of the protein sample in this reagent was then read at 595 nm. Each sample was analyzed twice and the protein concentrations were determined by comparing the average of the obtained OD values against BSA standard curve, generated by plotting the average of various absorbance versus various (known) concentrations of BSA.

2.11 Standard UV mutagenesis

Complete medium culture plates were incubated for 4 days at 37^{o}C. Conidiospores from 5 full plates were harvested in a sterile falcon containing 20 mL H_2O-Tween (0.02%) and vortexed. The solution was then filtered through blutex in a new falcon and more H_2O-Tween was added, until the final volume reached 40 mL. After vortexing, the solution was separated in two falcons and a final volume of 80 mL of the spore solution was equally distributed in 15-20 petri dishes, so that a very thin layer covered the bottom. The petri dishes were then exposed to UV light for 3 min 45 sec (the exposure time of the UV lamp was standardized after plotting a viability curve), all equally distanced from the UV light source. The solution from all petri dishes was quickly collected in two new falcons and centrifuged for 10 min at 4000 rpm. Only 20 mL of the supernatant were kept, and the rest was discarded. The pellets from both falcons were resuspended in the 20 mL and the final solution was poured into minimal medium (see Table 2.2) containing a nitrogen source (uric acid for this study), the necessary auxotrophies and 0.5% agar. After a quick vortexing, 5 mL of the TOP agar with the spores overlaid 20 already dried petri dishes containing minimal medium with the same supplements but 1% agar. After stabilization, all the petri dishes were incubated in 25^{o}C for 5-8 days. Specific mutants were isolated after streaking, due to their ability to grow in presence of uric acid as a sole nitrogen source. DNA extraction, PCR and finally sequencing of the whole gene of interest, helped us to locate the mutations caused by the UV exposure.

3. Results

3.1 C-terminally truncated Fur transporters (FurA-ΔC, FurD-ΔC and FurE-ΔC) are functional but FurE-ΔC shows an apparent modification in substrate specificity

Members of the Nucleobase Cation Symporter family 1 (NCS1) are present in prokaryotes, fungi and some plants. Fungal and especially *Aspergillus nidulans* NCS1 transporters, which have been extensively studied in respect to their function, specificity, regulation of expression and evolution, are classified into two distinct subfamilies, the Fcy-like and the Fur-like transporters (De Koning and Diallinas, 2000; Pantazopoulou and Diallinas, 2007; Krypotou *et al*., 2015a). *A. nidulans* possesses seven Fur transporters (FurA-G), two of which function as major uracil (FurD) or allantoin (FurA) transporters, one (FurE) is a secondary, lower-affinity, promiscuous transporter specific for uracil, allantoin and uric acid, while the rest are practically not expressed under laboratory conditions, but seem to be very low efficiency uracil transporters (Krypotou *et al*., 2015b).

Using functional GFP-tagged Fur versions, we have previously shown that the Fur transporters are differentially sensitive to endocytic turnover (Krypotou *et al*., 2015a), mostly evident in response to two well characterized endocytic triggers, those elicited by excess substrate or the presence of a primary nitrogen source (Gournas *et al*., 2010). In brief, FurE and FurF are highly sensitive to endocytosis, showing a degree of internalization and turnover even in the absence of endocytic signals (e.g. constitutive endocytosis), FurD is mostly sensitive to ammonium-elicited internalization, but less so to substrate-elicited endocytosis, whereas FurA is sensitive solely to ammonium-elicited endocytosis. Finally, FurC and FurG do not respond to any endocytic triggers.

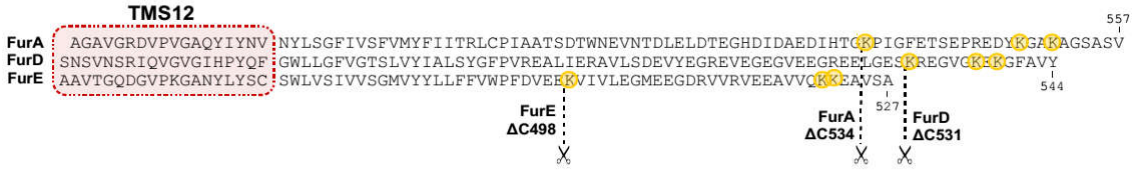

Figure 3.1 *Fur transporters C-terminal region alignment, where truncation sites and Lys residues as candidate ubiquitilation targets are marked.*

In order to investigate the basis of the differential response of Fur transporters to endocytosis, and based on the observation that all Fur proteins possess Lysine (Lys) residues as candidate ubiquitination targets at their C-terminal cytoplasmic region, we constructed and functionally analyzed strains expressing a truncated version of FurA, FurD or FurE transporter lacking its entire C-terminal region (Figure 3.1). We also constructed a C-terminally truncated version of a specific allele of FurE, FurE-K252F, which increases dramatically FurE-mediated transport activity and thus

permits better assessment of FurE function (Krypotou *et al*., 2015a). All truncated *fur* gene versions were fused C-terminally with the *gfp* orf, and the constitutive $gpdA_p$ promoter was used to drive their transcription.

The truncated Fur versions (named FurA-ΔC-GFP, FurD-ΔC-GFP, FurE-ΔC-GFP and FurE-K252F-ΔC-GFP) were introduced by standard genetic transformation in an *A. nidulans* strain lacking all major transporters specific for nucleobases, allantoin or nucleosides called Δ7, as it has been previously performed for the non-truncated FurA-GFP, FurD-GFP, FurE-GFP and FurE-K252F versions (Krypotou *et al*., 2015a). Selected purified transformants arising from intact single-copy plasmid integration events were analyzed further by growth tests, radiolabeled substrate uptake assays and epifluorescence microscopy.

Figure 3.2 shows a growth test of selected transformants and isogenic controls on minimal media (MM) containing uric acid or allantoin as sole nitrogen sources, or nitrate and toxic nucleobase analogues, known to be transported by the Fur transporters. As expected, a wild-type positive control strain grows on purines and allantoin and is sensitive to all nucleobase or nucleoside toxic analogues tested (e.g. 5FU, 5FC, 5FUd) as it expresses all relevant transporters. Also as expected, the negative control strain, Δ7, lacking all major nucleobase transporters, does not grow any uric acid or allantoin, and is resistant to toxic nucleobase/nucleoside analogues tested. It should be noted that Δ7 strain carries, among other transporter null mutations, total deletions of *furA* and *furD* genes, but has an intact *furE* gene. However, *furE* expression driven by its native promoter is extremely low so that no growth on uric acid or allantoin, or no sensitivity to 5FU, 5FC or 5FUd can be detected. This is only observed when FurE is expressed by the strong $gpdA_p$ promoter (Krypotou *et al*., 2015). Strains expressing the non-truncated GFP-tagged Fur versions by the $gpdA_p$ promoter confer distinct growth profiles on purines, allantoin or nucleobase toxic analogues, as follows. Strains expressing FurA grow on allantoin, albeit the relevant colonies are rather compact due to over-accumulation of this potentially toxic metabolite, and show increased sensitivity to 5FU. Strains expressing FurD grow moderately on uric acid and are highly sensitive to 5FU, 5FC or 5FUd. Strains expressing FurE or FurE-K252F grow on allantoin and uric acid, and are also differentially relatively sensitive to 5FU, 5FC or 5FUd. Similar growth phenotypes have been reported before (Krypotou *et al*., 2015). Strains expressing the corresponding truncated versions of FurA or FurD, (i.e. FurA-ΔC or FurD-ΔC) showed similar but not identical growth phenotypes with their non-truncated equivalents. In particular, the truncated FurD transporter shows slightly better growth on allantoin and is more resistant to 5FC than its non-truncated counterpart. More impressively, the strain expressing truncated FurE transporters (FurE-ΔC or FurE-K252F-ΔC) could not grow at all on uric acid, despite retaining the ability to grow on allantoin or being

sensitive to 5FU, 5FC or 5FUd. In other words, deletion of the C-terminal region of at least FurD and FurE/FurE-K252F led to an apparent modification of the substrate specificity of these transporters. The molecular rationale behind this observation is a major theme of this work.

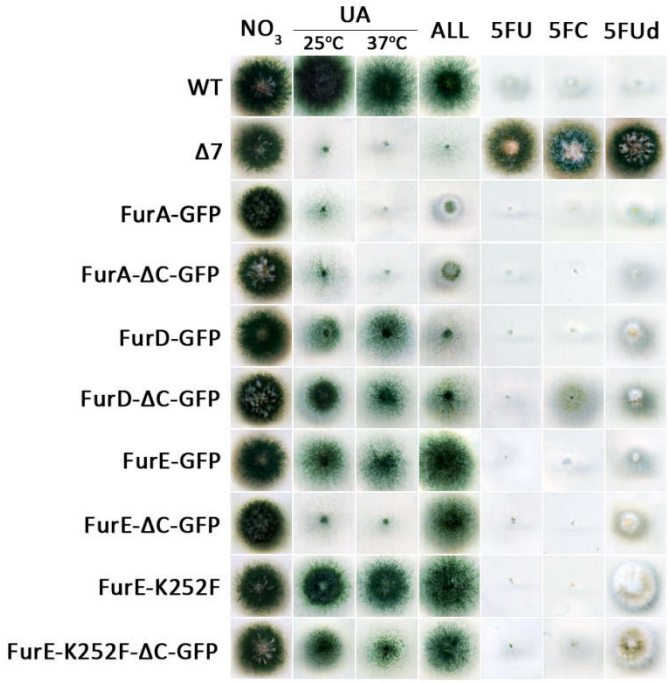

Figure 3.2 *Growth tests of transformants overexpressing truncated and non-truncated Fur transporters. The nitrogen sources or toxic analogues used are: nitrate (NO_3), uric acid (UA), allantoin (ALL), 5-fluorouracil (5FU), 5-fluorocytosine (5FC) and 5-fluorouridine (5FUd). Growth tests shown were performed at 37°C or 25°C when indicated. Toxic analogues were used in media containing nitrate as nitrogen source. A wild-type strain (WT) was used as a positive control and a Δ7 strain as a negative control (see text).*

3.2 C-terminally truncated Fur transporters show increased stability, due to blocking in their internalization and endocytic turnover

In order to investigate the effect of C-terminal truncation in Fur transporters, we followed the subcellular localization and turnover of the truncated versions by *in vivo* epifluorescence microscopic analysis. We tested both the rate of constitutive endocytosis and that of endocytosis triggered by either excess of substrate or the addition of a primary nitrogen source (e.g. ammonium). Figure 3.3A shows that in all cases, C-terminal truncation of the Fur proteins stabilizes the Fur transporters in the plasma membrane. As a consequence, very little, if any, fluorescence is associated with vacuoles, unlike what is observed in the non-truncated Fur versions. Vacuolar GFP fluorescence is a standard measure for detecting endocytosis of GFP-tagged transporters in fungi and mammalian cells, as transporters are internalized from the plasma membrane and are sorted into vacuoles via the endosomal/MVB pathway (Gournas *et al*., 2010). Once in the vacuolar lumen, GFP remains rather stable for a sufficient period of time, something that permits quantification of fluorescence (Gournas *et al*., 2010). To further support our conclusion on the role of the C-terminal region on Fur transporter stability, we performed quantification and

statistical analyses of endocytosis, as measured by estimating the surface and intensity of vacuolar GFP fluorescence. Our results, summarized in Figure 3.3B, confirm an absolutely essential, *cis*-acting role of the C-terminal region in the endocytosis of all Fur proteins. Western blot analysis using an anti-GFP antibody further confirmed that truncation of the C-terminal region increased dramatically the stability of FurE, as not only the steady state levels of intact FurE-ΔC-GFP were much higher than those of non-truncated FurE, but also the amount of free GFP was lower in FurE-ΔC-GFP versus FurE expressing strains (Figure 3.4A).

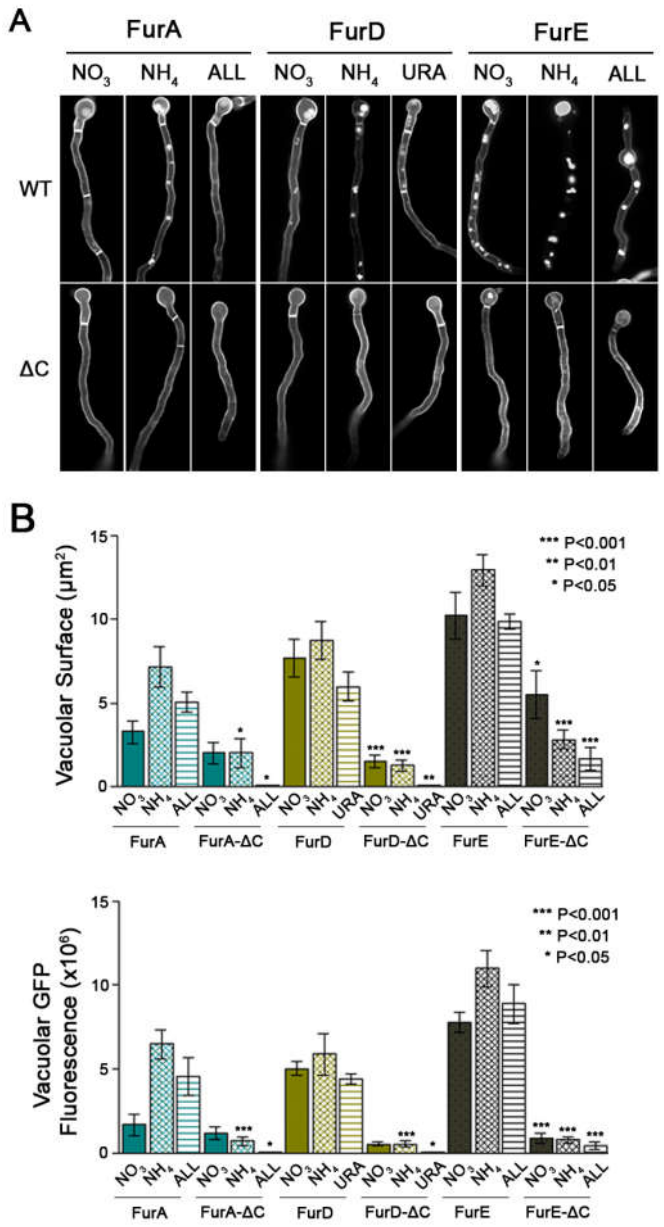

Figure 3.3 *In vivo subcellular localisation of Fur transporters and quantification of Fur transporters endocytosis.*

A. *Epifluorescence microscopy of GFP-tagged Fur proteins which are expressed by the strong gpdA promoter and display distinct relative internalization sensitivities in the presence of ammonium or substrate. Truncation of the C-terminal region stabilizes Fur transporters in the plasma membrane under all conditions tested. (ALL: allantoin, URA: uracil). Cultures were grown in MM for 16-18 h at 25°C.*

B. *Quantification and statistical analysis of transporters endocytosis by measuring vacuolar surface or vacuolar GFP fluorescence. Non-truncated transporters (controls) are compared to truncated transporters in each condition tested. Standard deviation is depicted with error bars. (n=5)*

Furthermore, we measured directly the transport activity of truncated versus non-truncated versions of FurD and FurE by standard uptake assays (Krypotou and Diallinas, 2014) using radiolabeled uracil (FurA activity cannot be assayed as there is no commercially available allantoin). Figure 3.4B shows that truncated FurD and FurE

had similar uptake rates (see values at 1 min uptake), albeit approximately 40-50% reduction of steady-state accumulation of uracil compared to the non-truncated equivalents, suggesting that the presence of the C-terminal region has a moderate, but still detectable reduction in the uptake capacity of Fur transporters. To further dissect the role of the C-tail of FurD and FurE in transport, we determined the K_m or K_i values of FurD-ΔC and FurE-K252F-ΔC (as described in Krypotou and Diallinas, 2014) for tentative substrates (uracil, uric acid, allantoin) and compared them with those of non-truncated FurD and FurE transporters (Figure 3.4C). This shows that truncation of FurD reduced the affinity for uracil (4.6-fold) and (> 10-fold) for uric acid. Contrastingly, truncation of FurE-K252F did not affect significantly the affinity for uracil and uric acid, and led to a moderate 2.5-fold reduction in allantoin binding. Overall, these results show that although truncation of the C-terminal region of Fur transporters increases their stability in the PM, it also differentially affects the relevant kinetics of transport.

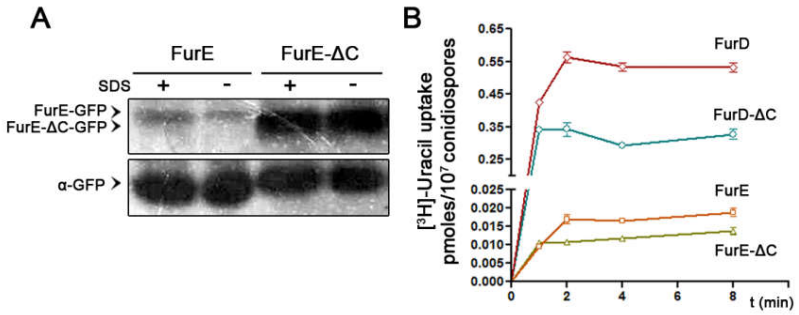

C

	K_m (μM)	K_i (μM)	
	UR	UA	ALL
FurD	0,78	99	>1000
FurD-ΔC	3,6	~1000	>1000
FurE	~1000	20	~1000
FurE-ΔC	n.m.	n.m.	n.m.
FurE K252F	8	80	56
FurE K252F-ΔC	9	76	128

Figure 3.4 A. *Western blot analysis of total protein extracts from strains expressing GFP-tagged FurE (control) and FurE-ΔC transporters from the* $gpdA_p$*, using anti-GFP antibody. Cultures were grown in MM supplemented with nitrate at 25°C for 16 h.* ***B.*** *Time courses of FurD-ΔC and FurE-ΔC-mediated [*^{3}*H]-uracil uptake, compared with the non-truncated FurD and FurE transporters activities respectively. Standard deviation is depicted with error bars.* ***C.*** $K_{m/i}$ *values (μM) for truncated and non-truncated FurD and FurE transporters were determined using [*^{3}*H]-uracil uptake competition. Results are averages of three measurements for each concentration point. Standard deviation was <20%. (n.m., non measurable).*

3.3 HulA ubiquitin ligase and specific Lysine residues in the extreme C-terminal region of Fur transporters are essential for their endocytosis

Our results strongly suggest that the C-terminal region of all transporters tested includes elements essential for endocytosis. In order to test whether internalization and turnover of Fur transporter takes place as a result of their prior modification by HulA-dependent ubiquitylation, as has been previously shown for other *A. nidulans* transporters (Karachaliou *et al*., 2013), we followed the subcellular localization of the GFP-tagged versions of FurA and FurD in the genetic background of conditional *hulAΔ* knockdown mutant, under endocytic and control conditions. The expression of *hulA*

gene was controlled by the *thiA* promoter, which means that in presence of thiamine, the expression of the gene is derepressed. Figure 3.5 shows that when HulA ubiquitin ligase expression is repressed, the endocytosis of all Fur proteins is totally blocked, so that they remain stably localized in the PM, under all conditions tested. Given that a similar stabilization was obtained when the Fur proteins were C-terminally truncated, the candidate Lys residues acting as acceptors of ubiquitin addition by HulA are probably located in the C-terminal cytoplasmic region of the Fur proteins. The truncated segments, in all cases, included three Lys residues, two very close to the terminal amino acid residue, and a third more distal. In order to test the role of these Lys, we constructed versions of all Fur proteins lacking their two extreme C-terminal Lys. In all cases, Lysines were replaced by Arg residues. These substitutions did not affect the function of Fur transporters, as judged by the relevant growth profiles of the relevant mutants on uric acid, allantoin or 5FU (Figure 3.6A). We subsequently followed the subcellular localization of the relevant mutants lacking these Lys residues under endocytic and control conditions. Figure 3.6B shows that all Fur versions lacking the two extreme C-terminal Lys residues were insensitive to internalization, and thus remained stably integrated in the PM, a result similar to the corresponding Fur truncations. Again, we performed quantification and statistical analyses of endocytosis, as shown in Figure 3.6C.

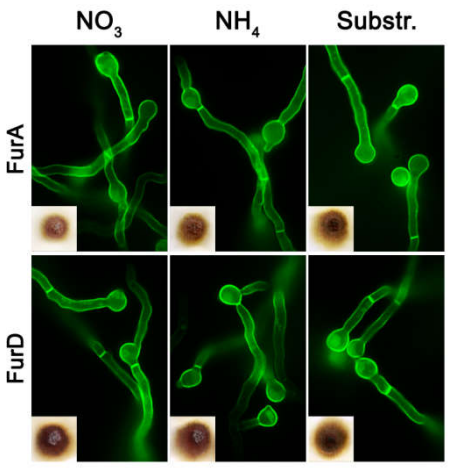

Figure 3.5. *Epifluorescence microscopy of GFP-tagged FurA and FurD expressed by the strong gpdA promoter in a genetic background of conditional hulAΔ knockdown mutant (see text). The endocytosis of all Fur proteins is totally blocked under all conditions tested. (substr.: allantoin for FurA and uracil for FurD). Cultures were grown in MM with 50 μM final concentration of thiamine for 16-18 h at 25°C. Phenotypes of the colonies under the same conditions are depicted in the bottom left panel.*

These results confirm that Fur endocytosis takes place via HulA-dependent ubiquitination of the most C-terminally located Lys residues of these transporters. This in turn suggests that the distinct sensitivities of Fur transporters to endocytic signals are very probably dependent on the different affinities that HulA adaptor proteins, such as α-arrestins (Karachaliou *et al*., 2013), might have for the C-tails of these transporters. However, given that we considered as extremely interesting and novel the apparent effect of the C-terminal cytoplasmic region on FurE function and specificity, the rest of this work was directed towards this finding.

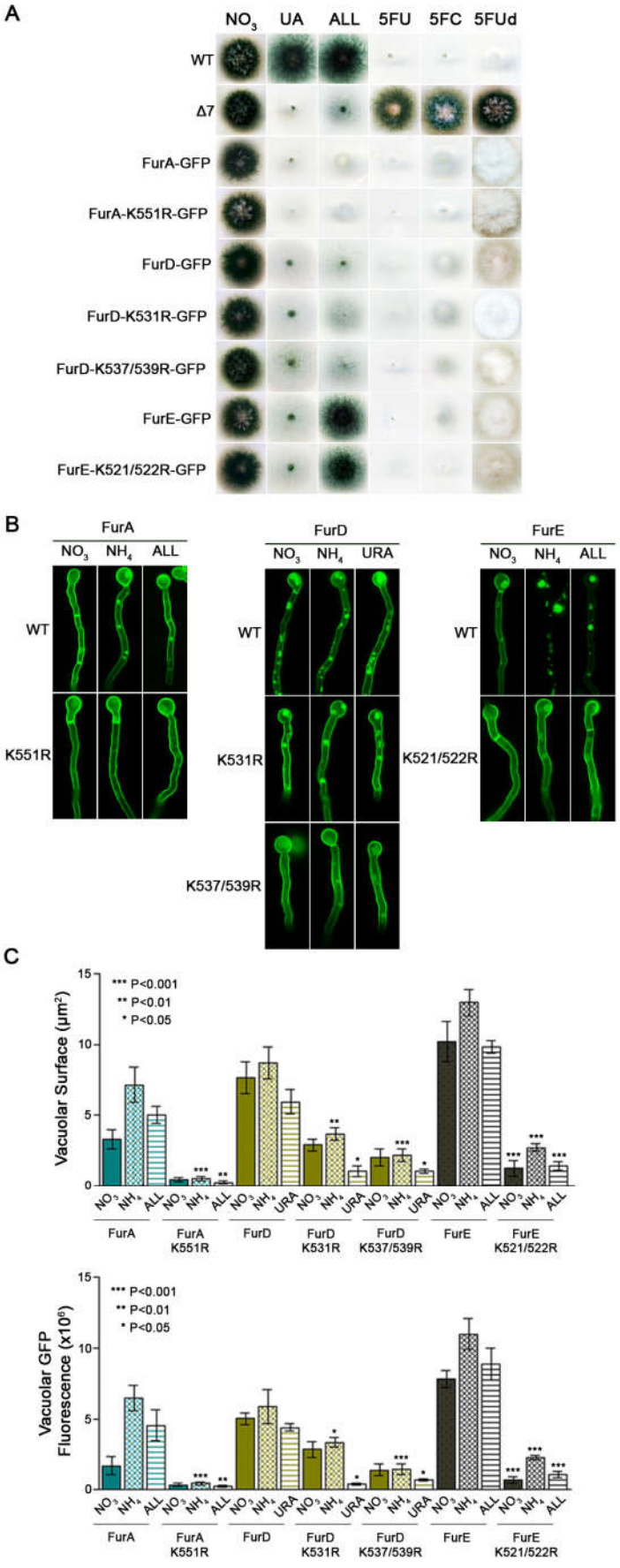

Figure 3.6 A. *Growth tests of transformants overexpressing transporters with mutations in specific Lys residues or non-truncated Fur transporters. The nitrogen sources or toxic analogues used are: nitrate (NO_3), uric acid (UA), allantoin (ALL), 5-fluorouracil (5FU), 5-fluorocytosine (5FC) and 5-fluorouridine (5FUd). Growth tests shown were performed at 37°C or 25°C when indicated. Toxic analogues were used in media containing nitrate as nitrogen source. A wild-type strain (WT) was used as a positive control and a Δ7 strain as a negative control.*

B. *Epifluorescence microscopy of GFP-tagged Fur proteins and mutants lacking specific Lys residues, expressed by the strong gpdA promoter. All mutants genetically lacking Lys were insensitive to internalization under all conditions tested (ALL: allantoin, URA: uracil). Cultures were grown in MM for 16-18 h at 25°C.*

C. *Quantification and statistical analysis of transporters endocytosis by measuring vacuolar surface or vacuolar GFP fluorescence. Non-truncated transporters (controls) are compared to the relevant mutants lacking specific Lys residues in each condition tested. Standard deviation is depicted with error bars. (n=5)*

3.4 Genetic suppressors of the C-terminal truncation restore substrate specificity in FurE

In order to better understand how the C-terminal region might affect FurE specificity, we selected genetic suppressors that restore substrate specificity in FurE by directly selecting for revertants on media containing uric acid as a sole nitrogen source, after standard UV mutagenesis of the strain expressing FurE-ΔC-GFP (see Materials and Methods). We obtained more than 50 revertants able to grow on uric acid and the furE-ΔC orf of 46 of them was amplified by PCR and then sequenced. In nearly all cases we detected a single codon change, while in a single case two nearby codons were modified. Table 3.1 summarizes the profile of the suppressor mutations obtained.

Table 3.1. *Profile of the suppressor mutations obtained after standard UV mutagenesis.*

Mutation	Codon change	Number of isolates	Location	Putative domain
D26N	GAC > AAC	1	N-tail/TMS1	internal gate
T133V	ACG > GTG	4	TMS3	binding site
G222K	GGG > AAG	1	L5	internal gate
	GGG > AAG	4		
N308T	AAC > ACC	7	L7	external gate
	AAC > ACA	1		
	AAC > ACT	1		
S296R	AGC >CGC	4	TMS7	internal gate
V343I	GTC > ATC	1	TMS8	binding site
I371L	ATC > CTC	1	TMS9	external gate
I371F	ATC > TTC	3	TMS9	external gate
I371P	ATC > CCC	1	TMS9	external gate
Y392N	TAC > AAC	6	TMS10	external gate
Y392C	TAC > TGC	5	TMS10	external gate
Y392E	TAC > GAA	1	TMS10	external gate
L394P	CTG > CCG	4	TMS10	external gate

Overall, suppressor mutations map in several transmembrane segments (TMS3, -7, -8, -9 and -10), but also in external loops L5 or L7, and in the N-terminal region. Growth tests of the relevant mutant strains showed that they are all able to grow on uric acid and allantoin, and that they are all sensitive to the toxic nucleobase analogues (Figure 3.7A). Interestingly, T133V, and to a less degree some of the other mutants (e.g. Y392N, Y392E, V343I), could also grow moderately on xanthine, which is not a substrate of either FurE or FurE-ΔC. None of the mutants has acquired the capacity to grow on other purines that are not substrates of Fur transporters, such as adenine, hypoxanthine or guanine (not shown). Thus, all suppressor mutations

restored the ability of FurE-ΔC to transport uric acid, but additionally, some specific mutations enlarged the FurE/FurE-ΔC specificity profile to include xanthine. Notably, the suppressor mutations neither affected the proper localization of FurE-ΔC in the plasma membrane (Figure 3.7B), nor resulted in cryo- or thermo-sensitive growth phenotypes on FurE-ΔC substrates (not shown). These latter findings strongly suggest that the suppressors did not affect the 3D folding or the overall stability of the transporter.

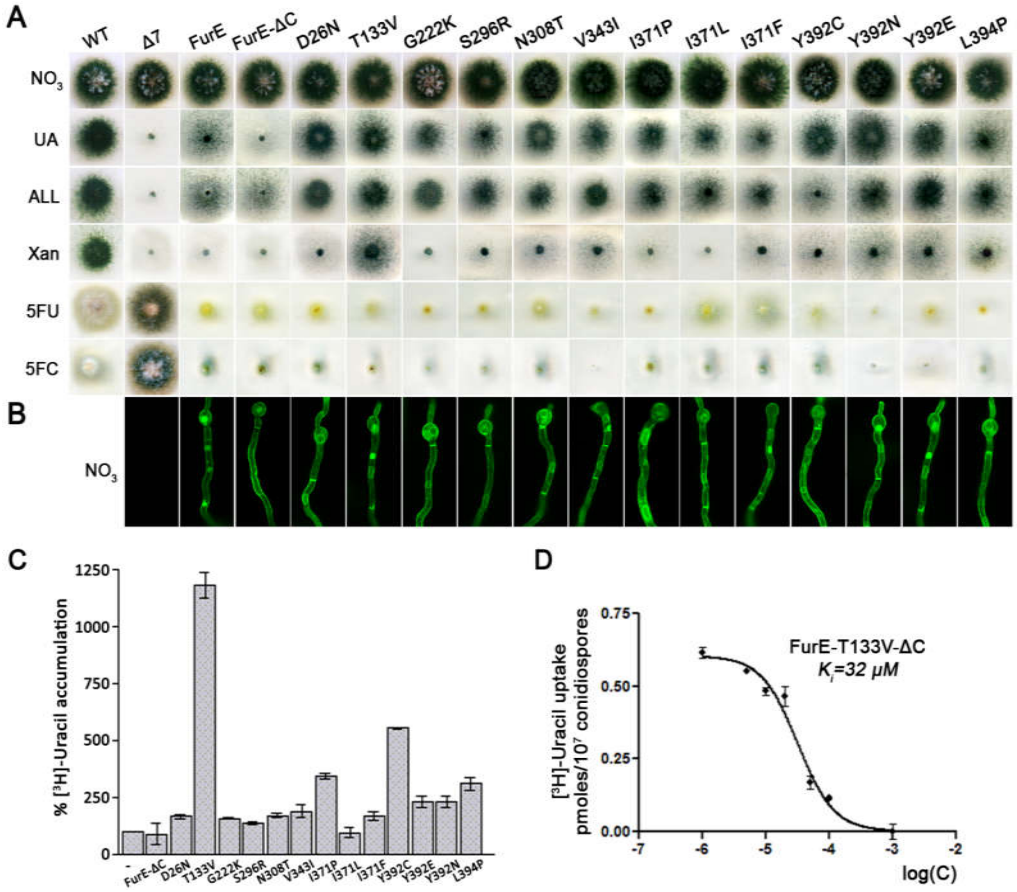

Figure 3.7. *Functional analysis of FurE-ΔC-GFP mutants.* ***A.*** *Growth tests of mutants overexpressing FurE-ΔC transporter. The nitrogen sources or the toxic analogues used are: nitrate (NO_3), uric acid (UA), allantoin (ALL), xanthine (Xan), 5-fluorouracil (5FU) and 5-fluorocytosine (5FC). Toxic analogues were used in media containing nitrate as a nitrogen source. All growth tests shown were performed at 37°C.* ***B.*** *Epifluorescence microscopy of the GFP-tagged FurE-ΔC mutants. The suppressor mutations do not seem to affect the proper localization of the transporter, in the plasma membrane. Cultures were grown in MM containing nitrate as nitrogen source for 16-18 h at 25°C.* ***C.*** *Comparative [^{3}H]-radiolabeled uracil accumulation for 4 min of FurE-ΔC mutants. Standard deviation is depicted with error bars* ***D.*** *Dose response curve of the FurE-T133V-ΔC-mediated [^{3}H]-uracil uptake in the presence of increasing concentration of non-radiolabelled uric acid, from which IC50 (equal to K_i in our analysis) of uric acid was measured. The specific mutation led to a 3-fold increase in uracil uptake.*

Comparative uptake assays further showed that most suppressors have little effect on the generally low rate or steady state of accumulation of radioactive uracil mediated by FurE or FurE-ΔC (Figure 3.7C). The most prominent exception was mutation T133V (in TMS3), which led to a >10-fold increase in uracil uptake, and to lower degree mutations I371P (TMS9) and Y392C (TMS10), which led to 3 to 6-fold increases. The generally low uracil uptake rates of most suppressors did not permit a rigorous estimation of affinity constants for FurE substrates, and thus we could not generally test whether suppressors re-conferred uric acid transport by increasing uric acid binding. The K_i for uric acid could only be measured for mutant FurE-T133V-ΔC, the only suppressor that showed sufficient transport activity for kinetic analysis. Figure 3.7D shows that FurE-T133V-ΔC has an affinity constant of 32 μM for uric acid. This value cannot be compared directly to the original truncated FurE-ΔC, since this has very low transport activity to be measured kinetically, but is similar to the K_i for uric acid of the non-truncated FurE (20 μM; see Figure 3.4C). Thus, in principle, we cannot exclude that the defect in FurE-ΔC was reduced affinity for uric acid, and that uric acid transport was regained because mutation T133V led to a prominent increase in uric acid binding. However, we consider this rather unlikely, given that C-terminal truncation of the hyperactive FurE-K252F version, where kinetics could be performed (see Figure 3.4C), has not affected the substrate affinity constants of any FurE substrate, including uric acid. This suggests that the ability of transporting specifically uric acid by different FurE versions does not seem to be related with the ability to bind or not uric acid.

Overall, the functional analysis of suppressors showed that the relevant mutations do not affect significantly the expression, folding, transport activity of uracil and turnover of FurE-ΔC, but specifically modify the ability of FurE-ΔC to transport uric acid. This observation suggested that suppressors might not affect the basic functional elements of FurE, including its major substrate binding-site, but rather affect peripheral domains acting as selectivity filters or gating elements controlling access to the binding site, as has been previously shown to be the case for the UapA uric acid-xanthine transporter (Papageorgiou *et al*. 2008; Diallinas 2014; Diallinas 2016), but also for FurD (Krypotou *et al*., 2015a).

3.5 Truncation of the FurE N-terminal region leads to growth phenotypes mimicking truncation of the C-terminal region

Given that one of the suppressors was located in the N-terminal region of FurE, we also constructed and studied two N-terminally truncated versions of the transporter (Figure 3.8). One of them, includes the entire N-terminal region along with some conserved motifs of unknown function in the NCS1 family. The second deletion includes the first 21 amino acid residues, which do not show an apparent

conserved segment in the NCS1 family. Both truncations, but mostly the shorter one, leads to loss of FurE-mediated transport of uric acid. Similarly to the C-terminal truncation, the N-terminal truncation did not seem to affect the ability of FurE to transport other recognized substrates of FurE, such as uracil, allantoin or toxic nucleobase/nucleoside analogues. In other words, both N- and C-terminal truncations of FurE lead to the same phenotype, with specific modification of substrate transport. The significance of this result is discussed later.

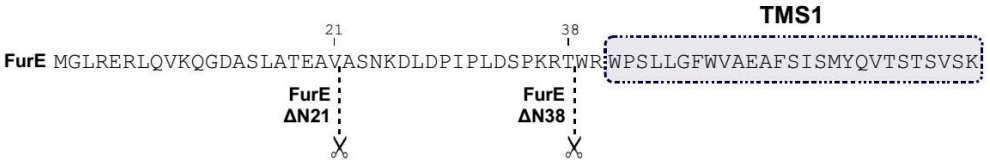

Figure 3.8. *FurE transporter N-terminal region, where truncation sites are marked.*

3.6 Suppressors reveal the critical role of distinct gating elements in FurE function and specificity

Fur transporters are homologous to the bacterial Mhp1 benzyl-hydantoin transporter, which also belongs to the NCS1 family. We have previously constructed and validated structural models of FurA, FurD and FurE based on the crystal structure of Mhp1. Validation included substrate docking, Molecular Dynamics and mutational analysis that alter the function or specificity of Fur transporters. This work has identified the putative binding site of relative substrates and has revealed the importance of TMS10, acting as an external gate critical for the high specificity of FurD (Krypotou *et al*., 2015a).

Herein, we mapped all characterized residues concerning suppressor mutations in the 3D model structure of FurE (Figure 3.9). Based on it, we could classify suppressors in three types (see also Table 3.1, Figure 3.9B-D). **Type I** suppressors concern amino acids proximal to substrate binding residues, as these were defined genetically, functionally and by *in silico* docking (Krypotou *et al*., 2015a). These are T133V (TMS3) and V342I (TMS8), which are very close to the major substrate binding residues Trp130 and Gln134 or Asn341, respectively. Thr133 seems to be an essential element of major binding site, whereas, Val341 lies “one step down” in the theoretical trajectory, from the binding site to the cytoplasm. **Type II** suppressors concern amino acids Ser296 in TMS7, Ile371 in TMS9, and Tyr392 and Leu394 in TMS10. TMS10 is a flexible transmembrane segment that has been shown to act as an outward-facing gate not only in FurD, but also in Mhp1 (Simmons *et al.,* 2014; Kazmier *et al*., 2014). More specifically, Molecular Dynamics have shown that TMS10 participates in an occlusion mechanism via its dramatic movement over the major substrate biding-site, while specific mutations in this segment modify (mostly enlarge)

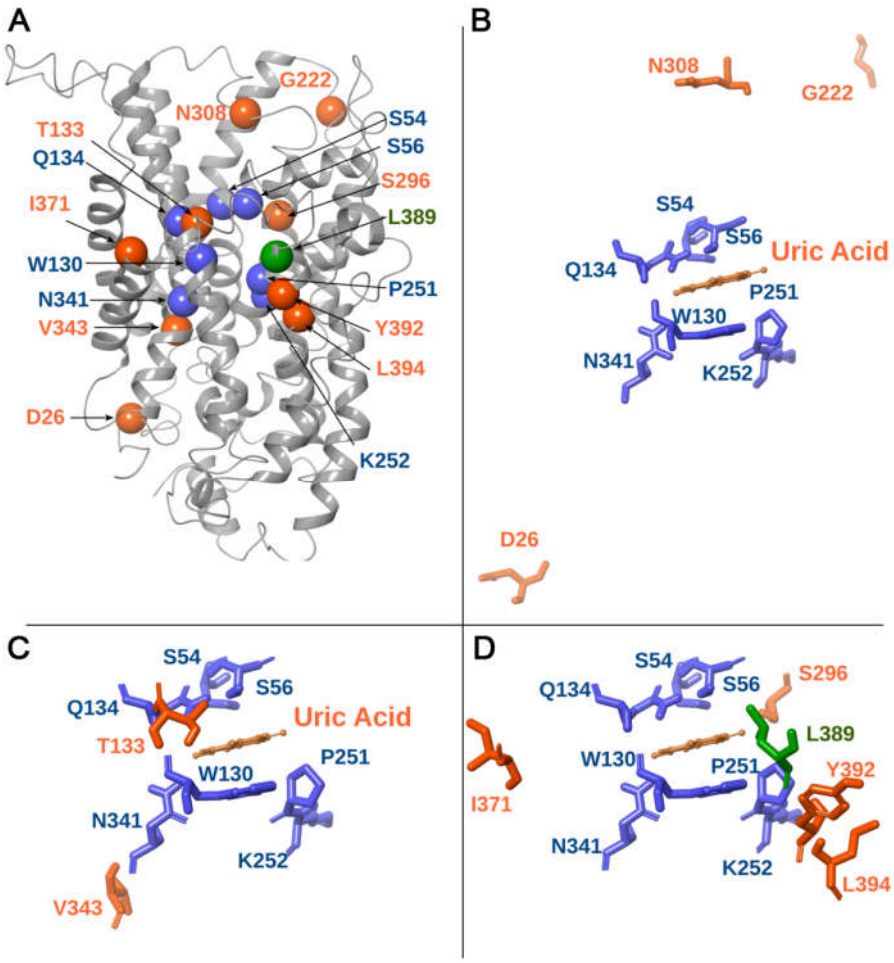

Figure 3.9. A. *3D model structure of FurE. The arrows indicate the location of the residues concerning suppressor mutations (see also Table 3.1).* ***B-D.*** *Type III, Type I and Type II suppressors respectively.*

the specificity of the transporters, apparently by compromising the occlusion mechanism (Shimamura *et al*., 2010; Adelman *et al*., 2011; Simmons *et al.,* 2014; Kazmier *et al*., 2014). This is highlighted in FurD, where mutation M389A converts this transporter from being highly specific for uracil, to a transporter capable of recognizing all purines and pyrimidines (Krypotou *et al*., 2015a). Also, in Mhp1, Leu363 plays a similar important role in substrate specificity (Simmons *et al.,* 2014). Furthermore, evidence from MDs in Mhp1 also suggests that TMS10 acts as outward-facing gate, in concert with TMS9 and the extracellular hydrophilic segment linking TMS7 and TMS8 (EL4 in Mhp1), the dynamics of which are very much dependent on substrate binding (Simmons *et al.,* 2014; Kazmier *et al*., 2014). Thus, the suppressors related to residues Ser296 in TMS7 and Ile371 in TMS9, could also affect the dynamics of an outward-facing gate in FurE. **Type III** suppressors concern amino acids located in flexible loops, distantly located form the substrate binding site. Asp26 is at the border of TMS1 with N-terminal cytoplasmic loop, Gly222 is in the extracellular loop L5, and Asn308 is in extracellular loop L7. Although there are no genetic or functional data related to these residues, MD in Mhp1 have shown that substrate

binding triggers the movement of TMS1, TMS5 and TMS7, consistent with the closing or opening of the intracellular (TMS1 and TMS5) and extracellular (TMS7) vestibules that lead to the major substrate binding-site (Simmons *et al*., 2014; Kazmier *et al*., 2014).

Overall, the suppressors isolated concern residues mapping either in or close to the major substrate binding-site (TMS3 and TMS8; Type I), or in an outward-facing gate (TMS7, TMS9, TMS10; Type II), or in dynamic loops that might act as hinges to control gating or the alteration form inward or outward and *vice versa* (N-terminal-TMS1, L5, L7; Type III).

4. Discussion

In the course of analyzing the functional role of the C-terminal cytoplasmic domain of *A. nidulans* Fur proteins, we came across an unexpected finding. The C-terminal cytoplasmic segment proved to be critical for the specificity of Fur transporters. The truncated FurD shows better growth on allantoin and is more resistant to 5-FC than its non-truncated counterpart. Kinetic analysis showed that FurD-ΔC has reduced affinity for uracil (5-fold) and uric acid (10-fold), which only partially explains the differences detected in apparent transport specificities, as this is detected by growth tests. More strikingly, the strains expressing the truncated FurE or FurE-K252F transporters showed none or reduced capacity for uric acid transport, while retaining their ability to transport allantoin, uracil and other nucleobase analogues. In this case, the specific loss or reduction of uric acid transport cannot be assigned to changes in affinity constants, as kinetic analysis showed that truncated and non-truncated versions, of at least FurE-K252F, have practically identical substrate binding affinities for all substrates, including uric acid. Thus, although truncation of the C-terminal region might affect the affinity of Furs for certain substrates, this cannot explain, in all cases, the apparent changes in specificity, best exemplified by the truncated versions of FurE. These findings indicated that C-terminal truncation might affect the specificity of Fur transporters without modifying its *bona fidae* substrate binding-site. Interestingly, we subsequently found that truncation of the N-terminal cytoplasmic region of FurE has a similar effect on specificity, that is, specific loss of uric acid transport. Thus, both cytoplasmic termini in FurE affect the substrate specificity, seemingly without affecting the substrate binding-site. These observations are in line with what we have proposed recently on the role of distinct gating elements, which act independently yet synergistically with the substrate binding-site, determining the specificity of members of the Fur family and other transporters (Diallinas, 2014; Krypotou *et al*., 2015; Alguel *et al*., 2016; Diallinas, 2016).

Using an unbiased genetic approach, we fortified our conclusion by selecting suppressors ‘correcting’ the loss of uric acid transport by the truncated FurE-ΔC transporter. After nearly saturated mutagenesis, we obtained suppressor mutations in residues located in the periphery of the substrate binding-site, in a tentative external gate, or in flexible loops that might act as hinges during conformational changes associated with transport catalysis. Notably, we did not obtain any mutations affecting residues proposed to bind substrates directly, which supports our previous notion that specificity in evolutionary and structurally similar transporters is principally determined by the so called gating elements or selectivity filters, and not by the substrate binding-site.

At present, the role of the C- and N-terminal cytoplasmic domains of FurE in substrate specificity is difficult to explain through a general mechanistic rationale. A mechanistic explanation becomes even more intriguing considering that truncation of the C-terminal region did affect the specificity of all Fur transporters similarly. In addition, bacterial Fur homologues lack extended N- and C-terminal cytoplasmic domains. However, our genetic analysis provided some hints on how this might be achieved, at least in specific transporters as is the case of FurE. Our results lead to the basic idea that the cytoplasmic N- and C-termini interact physically and thus affect the opening of an external gate and the positioning of specific residues, which act as selectivity filters, along the substrate translocation trajectory. The proper interaction of the N- and C-termini would promote the full, outward-facing, opening of the transporter and access of all physiological substrates to the major binding site. Upon substrate binding, induced fit conformational changes would disrupt the interactions of the N- and C-termini and promote the opening of the substrate binding-site intracellularly. We obtained direct evidence, by using an intragenic BiFC assay, that the N- and C-terminal cytoplasmic regions of FurE do come in close distance, and thus very probably interact. Contrastingly, we did not detect a BiFC positive signal when the two parts of split-YFP were cloned *in trans*, that is, into different FurE molecules (results not shown). This negative result might also signify that FurE molecules, and other NCS1 homologues, do not form stable dimers. This is in agreement with the monomeric structure of Mhp1 found in all crystals analyzed so far (Weyand *et al*., 2008; Simmons *et al*., 2014).

Interestingly, an analogous mechanism, proposing the interaction of cytoplasmic domains as important for the proper function of other transporters, has been shown to occur in prokaryotic ABC transporters or the homologous human CFTR chloride channel, which is involved in cystic fibrosis (Gadsby *et al*., 2006; Mihalyi *et al.* 2016). In particular, in CFTR and other ABC transporters, ATP-binding induced dimerization of two cytosolic nucleotide binding domains (NBDs) opens the pore, and dimer disruption following ATP hydrolysis closes it. Spontaneous openings without ATP are rare in wild-type, but not in mutants versions of CFTR, but still strictly coupled to NBD dimerization. Thus, coordinated NBD/pore movements are therefore intrinsic to CFTR suggesting that ATP alters the stability, but not the fundamental structural architecture of open and closed pore conformations even without ATP. The apparently cyclic, dynamic restructuring of the intramolecular domain made of two NBD domains might be mechanistically analogous to the N- and C-tail interaction, which we propose being at the basis of the gating cycle in FurE. In the case of Fur or other NCS1 transporters, the interaction of the N- and C-termini does not seem to be absolutely essential for the alternation of outward- and inward-facing conformations accompanying transport catalysis. This is concluded basically because cytoplasmic termini are not necessary for transport of some substrates (e.g allantoin or uracil)

and also, because prokaryotic homologues lack cytoplasmic termini altogether. It seems more probable that the interaction of the N- and C-termini finely regulates the opening and closing of gates, rather than the alternation of outward- and inward-facing conformations.

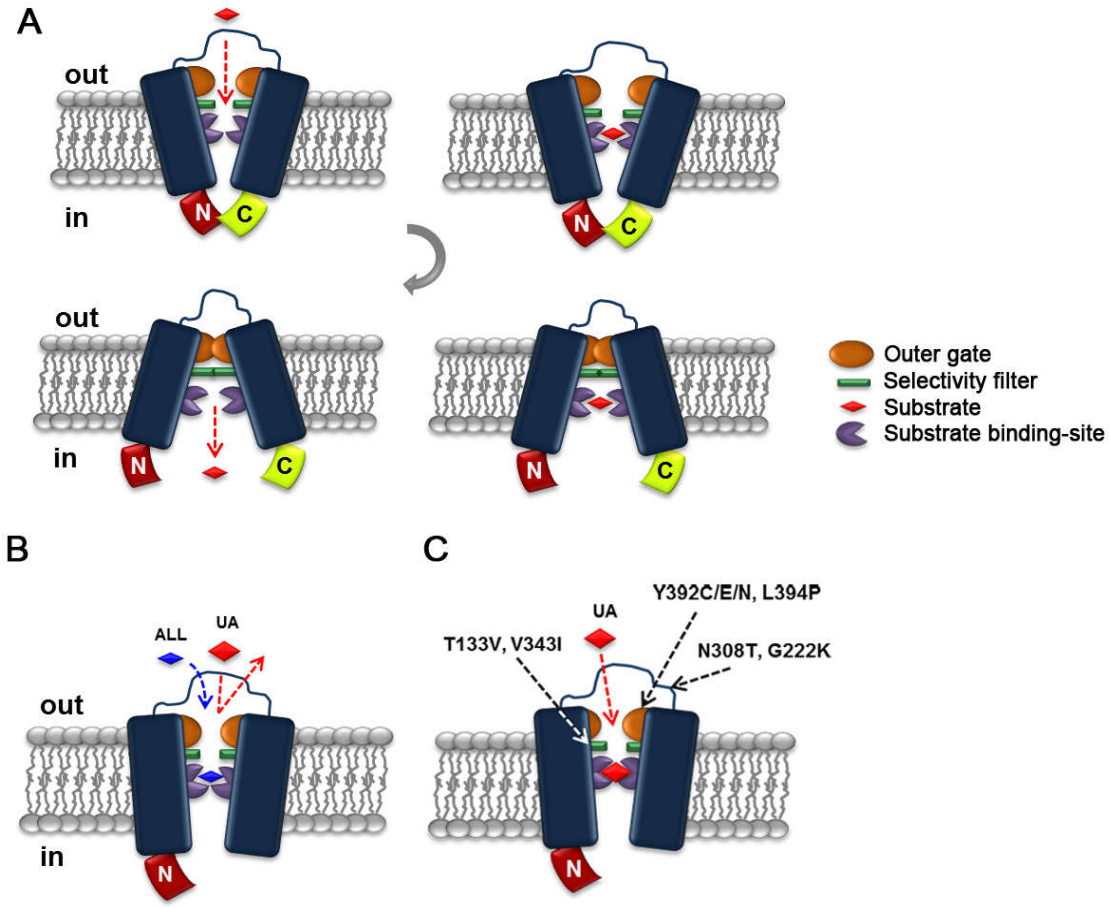

Figure 4.1. *Speculative model for the function of FurE.* ***A.*** *Starting from the top left, in the non-truncated version found in the outward-facing conformation, an interaction of the N- and C-termini opens 'fully' the external gate and thus all physiological substrates (uric acid, allantoin or uracil) fit and bind the major substrate binding. Proper substrate binding triggers occlusion of the outward-facing gate. Closing of the outward-facing gate elicits a gross conformational change leading to the inward-closed structure. This will subsequently disrupt of the N- and C-termini interaction, open the internal gate, and lead to release of substrate into the cytoplasm.* ***B.*** *C-terminus truncation leads to partial opening of the outer gate, blocking the access to uric acid but not to allantoin.* ***C.*** *Suppressor mutations modify gating elements, restoring the access of uric acid.*

In a speculative model for the functioning FurE (Figure 4.1), the order of events might be as follows: in the non-truncated version found in the outward-facing conformation, an interaction of the N- and C-termini fully opens the external gate and thus all physiological substrates (uric acid, allantoin or uracil) fit and bind the major substrate binding. Proper substrate binding triggers occlusion of the

outward-facing gate. Closing of the outward-facing gate elicits a gross conformational change leading to the inward-closed structure. This will subsequently disrupt of the N- and C-termini interaction, open the internal gate, and lead to release of substrate into the cytoplasm. Lack of the C- or N-terminal region alleviates the full opening of the external gate, in a way that only smaller or specific substrates (e.g. uracil and allantoin) can have access to the binding site. Thus, uric acid is excluded either because the external gate is not sufficiently open or because the closing of the gate is not the proper one. Suppressor mutations affect the gates directly so that they regain their proper opening and closing that accommodates uric acid and permits its transport. Although we support an interaction of the N- and C-termini, we cannot exclude that they function independently and control the gating mechanism.

Last but not least, our work also revealed the importance of specific C-terminally located Lys residues in HulA-dependent ubiquitination and turnover of all Fur transporters, a case similar to what has been found for the UapA uric acid/xanthine transporter, representing the other major nucleobase transporter family in fungi. Given, however, the prominent differences in the rate of endocytic turnover of distinct Fur transporters, it will be worth trying to identify the molecular basis of such differences, and in particular to investigate the role of the nine different arrestin-like adaptors (Karachaliou *et al*. 2013) in the endocytosis of NCS1 transporters.

5. References

Adelman, J. L., A. L. Dale, M. C. Zwier, D. Bhatt, L. T. Chong *et al.*, 2011 Simulations of the alternating access mechanism of the sodium symporter Mhp1. Biophys J. 101(10): 2399-407.

Alberts, B., D. Bray, J. Lewis, M. Raff, K. Roberts *et al.*, 1994 Membrane Structure. In Molecular Biology of the Cell. Garland Publishing, New York.

Alexopoulos, C. J., C. W. Mims, and M. Blackwell, 1996 Introductory Mycology. 4th ed., John Wiley and Sons, New York.

Alguel, Y., A. D. Cameron, G. Diallinas, B. Byrne, 2016 Transporter oligomerization: form and function. Biochem Soc Trans. 44(6): 1737-1744.

Alguel, Y., S. Amillis, J. Leung, G. Lambrinidis, S. Capaldi *et al.*, 2016 Structure of eukaryotic purine/H^+ symporter UapA suggests a role for homodimerization in transport activity. Nat Commun. 7: 11336.

Amillis, S., Z. Hamari, K. Roumelioti, C. Scazzocchio, and G. Diallinas, 2007 Regulation of expression and kinetic modelling of substrate interactions of a uracil transporter in *Aspergillus nidulans*. Mol Membr Biol. 24: 206–214.

Apte-Deshpande, A., S. Rewanwar, P. Kotwal, V. A. Raiker, S. Padmanabhan, 2009 Efficient expression and secretion of recombinant human growth hormone in the methylotrophic yeast *Pichia pastoris*: potential applications for other proteins. Biotechnol Appl Biochem. 54(4): 197-205.

Berbee, M. L., 2001 The phylogeny of plant and animal pathogens in the Ascomycota. Physiol Mol Plant Pathol. 59: 165-187.

Bradford, M. M., 1976 A rapid and sensitive method for the quantitation of microgram quantities of protein utilizing the principle of protein-dye binding. Anal Biochem. 72:248-54.

Casselton, L., and M. Zolan, 2002 The art and design of genetic screens: filamentous fungi. Nat Rev Genet. 3(9): 683-97.

Colas, C., P. M. Ung, A. Schlessinger, 2016 SLC Transporters: Structure, Function, and Drug Discovery. Med. Chem. Commun. 7(6): 1069–1081.

Cove, D. J., 1966 The induction and repression of nitrate reductase in the fungus *Aspergillus nidulans*. Biochim Biophys Acta. 113(1): 51-6.

Darlington, A. J., and C. Scazzocchio, 1967 Use of Analogues and the Substrate-Sensitivity of Mutants in Analysis of Purine Uptake and Breakdown in Aspergillus nidulans. J Bacteriol. 93: 937-940.

Diallinas, G., 2014 Understanding transporter specificity and the discrete appearance of channel-like gating domains in transporters. Front Pharmacol. 5: 207.

Diallinas, G., 2016 Dissection of Transporter Function: From Genetics to Structure. Trends Genet. 32(9): 576-90.

Drew, D., and O. Boudker, 2016 Shared molecular mechanisms of membrane transporters. Annu. Rev. Biochem. 85: 543–572.

Dupré, S., D. Urban-Grimal, R. and Haguenauer-Tsapis, 2004 Ubiquitin and endocytic internalization in yeast and animal cells. Biochim Biophys Acta. 169: 89–111.

Engel, A., and H. E. Gaub, 2008 Structure and mechanics of membrane proteins. Annu Rev Biochem. 77: 127-48.

Esser, K., and U. Stahl, 1976 Cytological and genetic studies of the life cycle of Saccharomycopsis lipolytica. Mol Gen Genet. 146(1): 101-6.

Forrest, L. R., R. Krämer, C. Ziegler, 2011 The structural basis of secondary active transport mechanisms. Biochim Biophys Acta. 1807(2): 167-88.

Gadsby, D.C., P. Vergani, L. Csanády, 2006 The ABC protein turned chloride channel whose

failure causes cystic fibrosis. Nature. 440(7083): 477-83.

Galanopoulou, K., C. Scazzocchio, M. E. Galinou, W. Liu, F. Borbolis et al., 2014 Purine utilization proteins in the Eurotiales: cellular compartmentalization, phylogenetic conservation and divergence. Fungal Genet Biol. 69: 96–108.

Gournas, C., S. Amillis, A. Vlanti, and G. Diallinas, 2010 Transport-dependent endocytosis and turnover of a uric acid-xanthine permease. Mol Microbiol. 75: 246–260.

Hamari, Z., S. Amillis, C. Drevet, A. Apostolaki, C. Vágvölgyi *et al.*, 2009 Convergent evolution and orphan genes in the Fur4p-like family and characterization of a general nucleoside transporter in *Aspergillus nidulans*. Mol Microbiol. 73: 43–57.

Houbraken, J., R. P. de Vries, R. A. Samson, 2014 Modern taxonomy of biotechnologically important *Aspergillus* and *Penicillium* species. Adv Appl Microbiol. 86:199-249.

Jund, R., E. Weber, and M. R. Chevallier, 1988 Primary structure of the uracil transport protein of Saccharomyces cerevisiae. Eur J Biochem. 171: 417–424.

Kaback, H. R., I. Smirnova, V. Kasho, Y. Nie, Y. Zhou, 2011 The alternating access transport mechanism in LacY. J Membr Biol. 239(1-2): 85-93.

Karachaliou, M., S. Amillis, M. Evangelinos, A. C. Kokotos, V. Yalelis et al., 2013 The arrestin-like protein ArtA is essential for ubiquitination and endocytosis of the UapA transporter in response to both broad-range and specific signals. Mol Microbiol. 88: 301–317.

Kazmier, K., S. Sharma, S. M. Islam, B. Roux, H. S. Mchaourab, 2014 Conformational cycle and ion-coupling mechanism of the Na^+/hydantoin transporter Mhp1. Proc Natl Acad Sci U S A. 111(41): 14752-7.

Kirk, P. M., P. F. Cannon, D. W. Minter, and J. A. Stalpers, 2008 Dictionary of the Fungi. 10th ed., Wallingford: CABI.

Kjeldsen, T., 2000 Yeast secretory expression of insulin precursors. Appl Microbiol Biotechnol. 54: 277-286.

Klingenberg, M., 2007 Transport viewed as a catalytic process. Biochimie. 89: 1042–1048.

Kosti, V., I. Papageorgiou, and G. Diallinas, 2010 Dynamic elements at both cytoplasmically and extracellularly facing sides of the UapA transporter selectively control the accessibility of substrates to their translocation pathway. J Mol Biol. 397: 1132–1143.

Koukaki, M., E. Giannoutsou, A. Karagouni, and G. Diallinas, 2003 A novel improved method for *Aspergillus nidulans*transformation. J Microbiol Methods. 55: 687–695.

Krypotou, E., V. Kosti, S. Amillis, V. Myrianthopoulos, E. Mikros *et al.*, 2012 Modelling, substrate docking, and mutational analysis identify residues essential for the function and specificity of a eukaryotic purinecytosine NCS1 transporter. J Biol Chem. 287: 36792–36803.

Krypotou, E., and G. Diallinas, 2014 Transport assays in filamentous fungi: kinetic characterization of the UapC purine transporter of Aspergillus nidulans. Fungal Genet Biol. 63: 1–8.

Krypotou, E., C. Scazzocchio, and G. Diallinas, 2015 Functional characterization of NAT/NCS2 proteins of *Aspergillus brasiliensis* reveals a genuine xanthine-uric acid transporter and an intrinsically misfolded polypeptide. Fungal Genet Biol. 75: 56–63.

Krypotou, E., T. Evangelidis, J. Bobonis, A. A. Pittis, T. Gabaldón *et al.*, 2015 Origin, diversification and substrate specificity in the family of NCS1/FUR transporters. Mol Microbiol. 96(5): 927-50.

de Koning, H., and G. Diallinas, 2000 Nucleobase transporters. Mol Membr Biol. 17: 75–94.

Lauwers, E., Z. Erpapazoglou, R. Haguenauer-Tsapis, and B. André, 2010 The ubiquitin code of yeast permease trafficking. Trends Cell Biol. 20: 196–204.

Lockington, R. A., H. M. Sealy-Lewis, C. Scazzocchio, R. W. Davies, 1985 Cloning and characterization of the ethanol utilization regulon in *Aspergillus nidulans*. Gene.

33(2): 137-49.

Luckey, M., 2008 Membrane structural biology: with biochemical and biophysical foundations. Cambridge University Press.

Lutzoni, F., F. Kauff, C. J. Cox, D. McLaughlin, G. Celio et al., 2004 Assembling the fungal tree of life: progress, classification, and evolution of subcellular traits. Am J Bot. 91: 1446-1480.

Mihályi, C., B. Töröcsik, L. Csanády, 2016 Obligate coupling of CFTR pore opening to tight nucleotide-binding domain dimerization. Elife. 5.

Miranda, M., and A. Sorkin, 2007 Regulation of Receptors and Transporters by Ubiquitination: New insights into surprisingly similar mechanisms. Mol Interv. 7: 157-167.

Mirza, O., L. Guan, G. Verner, S. Iwata, H. R. Kaback, 2006 Structural evidence for induced fit and a mechanism for sugar/H^+ symport in LacY. EMBO J. 25: 1177–1183.

Pantazopoulou, A., and G. Diallinas, 2007 Fungal nucleobase transporters. FEMS Microbiol Rev. 31: 657–675.

Papageorgiou, I., C. Gournas, A. Vlanti, S. Amillis, A. Pantazopoulou *et al.*, 2008 Specific interdomain synergy in the UapA transporter determines its unique specificity for uric acid among NAT carriers. J Mol Biol. 382: 1121–1135.

Penmatsa, A., and E. Gouaux, 2014 How LeuT shapes our understanding of the mechanisms of sodium-coupled neurotransmitter transporters. J. Physiol. 592: 863–869.

Quistgaard, E. M., C. Löw, F. Guettou, P. Nordlund, 2016 Understanding transport by the major facilitator superfamily (MFS): structures pave the way. Nat Rev Mol Cell Biol. 17(2): 123-32.

Salom, D., and K. Palczewski, 2011 Structural Biology of Membrane Proteins. In Production of Membrane Proteins: Strategies for Expression and Isolation. Robinson, A. S. (ed.). Wiley-VCH Verlag Gmb & Co, pp. 249-273.

Sambrook, J., E. F. Fritsch, and T. Maniatis, 1989 Molecular Cloning: A Laboratory Manual, Second ed. NY: Cold Spring Harbor Laboratory, Cold Spring Harbor.

Sambrook, J., and D. W. Russel, 2001 Molecular Cloning: A Laboratory Manual, Third ed. NY: Cold Spring Harbor Laboratory, Cold Spring Harbor.

Scazzocchio, C., N. Sdrin, and G. Ong, 1982 Positive regulation in a eukaryote, a study of the uaY gene of *Aspergillus nidulans*: I. Characterization of alleles, dominance and complementation studies, and a fine structure map of the uaY-oxpA cluster. Genetics. 100(2): 185-208.

Scazzocchio, C., 2006 Aspergillus genomes: secret sex and the secrets of sex. Trends Genet. 22(10): 521-5.

Scazzocchio, C., 2009 Aspergillus: A Multifaceted Genus. In Encyclopedia of Microbiology, Schaechter, M. (ed.). Elsevier, Oxford. Pp. 401-421.

Schoch, C. L., G. H. Sung, F. López-Giráldez, J. P. Townsend, J. Miadlikowska et al., 2009 The Ascomycota tree of life: a phylum-wide phylogeny clarifies the origin and evolution of fundamental reproductive and ecological traits. Syst Biol. 58(2): 224-39.

Shi, Y., 2013 Common folds and transport mechanisms of secondary active transporters. Annu Rev Biophys. 42: 51-72.

Shimamura, T., S. Weyand, O. Beckstein, N. G. Rutherford, J. M. Hadden *et al.*, 2010 Molecular basis of alternating access membrane transport by the sodium-hydantoin transporter Mhp1. Science. 328(5977): 470-3.

Simmons, K. J., S. M. Jackson, F. Brueckner, S. G. Patching, O. Beckstein et al., 2014 Molecular mechanism of ligand recognition by membrane transport protein, Mhp1. EMBO J. 33(16): 1831-44.

Sioupouli, G., G. Lambrinidis, E. Mikros, S. Amillis, G. Diallinas, 2017 Cryptic purine transporters in Aspergillus nidulans reveal the role of specific residues in the

evolution of specificity in the NCS1 family. Mol Microbiol. 103(2): 319-332.

Todd, R. B., M. A. Davis, M. J. Hynes, 2007 Genetic manipulation of *Aspergillus nidulans*: meiotic progeny for geneticanalysis and strain construction. Nat Protoc. 2(4): 811-21.

Valdez-Taubas, J., L. Harispe, C. Scazzocchio, L. Gorfinkiel, A. L. Rosa, 2004 Ammonium-induced internalisation of UapC, the general purine permease from *Aspergillus nidulans*. Fungal Genet Biol. 41(1): 42–51.

Vlanti, A., and G. Diallinas, 2008 The *Aspergillus nidulans*FcyB cytosine-purine scavenger is highly expressed during germination and in reproductive compartments and is downregulated by endocytosis. Mol Microbiol. 68: 959–977.

Weber, E., C. Rodriguez, M. R. Chevallier, and R. Jund, 1990 The purine-cytosine permease gene of Saccharomyces cerevisiae: primary structure and deduced protein sequence of the FCY2 gene product. Mol Microbiol. 4: 585–596.

Weyand, S., T. Shimamura, S. Yajima, S. Suzuki, O. Mirza et al., 2008 Structure and molecular mechanism of a nucleobase-cation-symport-1 family transporter. Science. 322(5902): 709-13.

Yildirim, M. A.,K. L. Goh, M. E. Cusick, A. L. Barabás, M. Vidal, 2007 Drug-target network. Nat Biotechnol. 25(10): 1119-26.

6. Appendix

Oligonucleotides used in this study

Table 6.1. *Oligonucleotides used in this study.*

Oligonucleotide	5'-3' Sequence
GFP NotI R	CGC**GCGGCCGC**TTACTTGTACAGCTCGTCC
GFP PstI R	AA**CTGCAG**TTACTTGTACAGCTCGTCCATGC
FurD SpeI F	GCG**ACTAGT**ATGCGTTTCGGTCGCTTTCACC
FurA SpeI F	GCG**ACTAGT**ATGTCAGCTATTAAACGATGGATC
FurC SpeI F	GCG**ACTAGT**ATGGACCGCCTCTCCATCAG
FurE SpeI F	GCG**ACTAGT**ATGGGACTACGAGAAAGACTCC
FurA K534 NS NotI R	GCG**GCGGCCGC**GCCGGTGTGGATATCTTCCG
FurD K531 NS NotI R	GCG**GCGGCCGC**GCTCTCCCCCAACTCCTCCC
FurE K498 NS NotI R	GCG**GCGGCCGC**CTCTTCAACATCAAACGGCCAG
FurE ΔC509 NS NotI R	GCG**GCGGCCGC**TCCCTCCTCCATTCCCTCAAGCAC
FurC-FurE NS NotI R	GGG**GCGGCCGC**GACAGCCTCCTTCTTAACCTCCCTAACTCCAACC
gpdA (1000) AatII F	GCG**GACGTC**GGTTGACCGGTGCCTGGATC
YFPn XbaI F2	CGCG**TCTAGA**ATGGTGAGCAAGGGCGAGGAGCTG
YFPn SpeI R	CGCG**ACTAGT**TTACATGATATAGACGTTGTGGCTGTTG
FurD BglII F	GCCG**AGATCT**ATGCGTTTCGGTCGCTTTCACC
FurD XbaI NS R	GCGC**TCTAGA**TAAACAGCAAAACCCTTCTCC
FurE BamHI F	GCCG**GGATCC**ATGGGACTACGAGAAAGACTCC
FurE XbaI NS R	GCGC**TCTAGA**GCAGAGACAGCCTCCTTCTTCTGCACC
FurEN21 SpeI F	CGCG**ACTAGT**ATGGCCTCCAACAAAGACCTCG
FurEN38 SpeI F	CGCG**ACTAGT**ATGTGGAGATGGCCGTCACTAC
GFP NotI dstr F	GACGAGCTGTACAAGTAAGCGAACGCGATCCACTTAACGTTACTG
GFP NotI dstr R	CAGTAACGTTAAGTGGATCGCGTTCGCTTACTTGTACAGCTCGTC
FurE K498 XbaI R	GCG**TCTAGA**CTACTCTTCAACATCAAACGGCCAGAC
gpdA NotI F	GCG**GCGGCCGC**GCATGCCATTAACCTAGGTACAGAAGTCC
FurE seq 1	CGCCGTCTTCGGTATGCTTCC
FurE seq 2	CGCGGTACGCCAAAACTCCCAG
FurA K551R F	CGTGAAGATTATAAAGGTGCTCGAGCTGGATCCGCTAGTGTAGCG
FurA K551R R	CGCTACACTAGCGGATCCAGCTCGAGCACCTTTATAATCTTCACG
FurD K531R F	GGGAGGAGTTGGGGGAGAGTCGACGAGAAGGCGTTGGGAAGGAG
FurD K531R R	CTCCTTCCCAACGCCTTCTCGTCGACTCTCCCCCAACTCCTCCC
FurD K537_539R F	GAGAGAAGGCGTTGGGAGGGAGAGGGGTTTTGCTGTTTAC
FurD K537_539R R	GTAAACAGCAAAACCCCTCTCCCTCCCAACGCCTTCTCTC
FurD K531 on 537/539R F	GGGAGGAGTTGGGGGAGAGTCGACGAGAAGGCGTTGGGAGGGAGAGG
FurD K531 on 537/539R R	CCTCTCCCTCCCAACGCCTTCTCGTCGACTCTCCCCCAACTCCTCCC
FurE K521_522R F	GTTGAGGAGGCGGTGGTGCAGAGGAGGGAGGCTGTCTCTGCA
FurE K521_522R R	TGCAGAGACAGCCTCCCTCCTCTGCACCACCGCCTCCTCAAC